TEXTURAL ADJUSTMENTS DURING REGIONAL METAMORPHISM

THESIS FOR THE DEGREE OF M. S.

MICHIGAN STATE UNIVERSITY

MICHAEL PATRICK RYAN

1973

ABSTRACT

TEXTURAL ADJUSTMENTS DURING REGIONAL METAMORPHISM

by

Michael Patrick Ryan

Petrographic thin sections of regionally-metamorphosed Thunderhead Sandstone have received quantitative textural evaluation. Interior and exterior components of surface area vol.$^{-1}$ have been measured for quartz and plagioclase phases from 24 sites over the regional gradient. Statistical testing of components of variance within and between sampling sites indicate that quartz surface area components are very sensitive to local (outcrop-scale) conditions while plagioclase surface area is more responsive to regional effects. The textural mosaics formed by phase association were next modeled as states in a Markov chain. For non-collapsed chains, grain size variation in quartz and alkali feldspar influenced the amount of Markovity or determinism in the rock texture. Removal of grain size effects by chain collapsing suggested that a limiting value exists for the strength of neighborhood phase associations, and that the amount of site-to-site variation in determinism decreases with distance up the metamorphic gradient.

TEXTURAL ADJUSTMENTS DURING REGIONAL METAMORPHISM

By

Michael Patrick Ryan

A Thesis

Submitted to
Michigan State University
in partial fulfillment of the requirements
for the degree of

Master of Science

Department of Geology

1973

ACKNOWLEDGEMENTS

I thank Dr. Thomas A. Vogel for introducing me to rock textural problems and for providing guidance in the development of the research.

Dr. Charles Spooner kindly machined my "spinner randomizer" for use on a petrographic microscope stage.

My wife Masako was a constant source of encouragement, and deserves special thanks.

TABLE OF CONTENTS

LIST OF TABLES

LIST OF FIGURES

Page No.

INTRODUCTION

Ehrlich et al. (1972) have discussed the general concept of rock texture in regional metamorphism and the information textural parameters can carry. They demonstrated that the surface area and the shape of plagioclase grains are highly responsive to changes in metamorphism. Moreover, in the metamorphosed granodiorite they studied, these textural variables proved more responsive to metamorphic conditions than compositional variables.

This paper represents a further attempt to evaluate the response of selected textural variables to changes in the metamorphic environment.

Allen and Ragland (2) have reported chemical as well as textural variation in the Thunderhead Sandstone, from Gatlingburg, Tennessee to Cherokee, North Carolina. The Thunderhead Sandstone is a regionally metamorphosed arkose, of medium-to-coarse grain size. It is Precambrian in age, and is believed to have undergone prograde metamorphism in the Devonian, following overthrusting into its present location during the Ordovician (3).

A number of factors suggested using the Thunderhead Sandstone as a testing area for further textural work:

1) Relative homogeneity in composition

2) A facies range from greenschist to upper amphibolite

3) Massive bedding and numerous roadcuts made possible an adequate sampling plan

4) Lack of appreciable penetrative deformation

There are important similarities and differences between the Thunderhead Sandstone used for this study, and the Cross Lake Gneiss of Ontario used for a prior textural study (4). Both bodies have undergone prograde regional metamorphism from west to east within a distance of 20-25 miles, and in both cases, metamorphism ranged from greenschist to amphibolite facies. Differences between the Thunderhead (a meta-arkose) and the Cross Lake Gneiss (a meta-granodiorite) are compositional and textural. Modal composition in the Thunderhead Sandstone is 36% to 66% quartz, about 25% plagioclase, and an average of 21% micas, of which biotite predominates. The compsoition of the Cross Lake Gneiss is approximately 24% quartz, 54% plagioclase, 12% biotite and 2% muscovite (4). In the Thunderhead Sandstone, exposures in greenschist grade have preserved relict sedimentary textures, including graded bedding and cross bedding. In the Cross Lake Gneiss, primary igneous textures are preserved in the low-grade sector, including parallel alignment of plagioclase (4).

Rock textures may be specified by examination of two broad variable groups: grain boundary-based variables and grain aggregate-based variables. This paper will use surface area per unit volume--

a boundary parameter and phase mosaic patterns--a grain aggregate parameter, to quantitatively test the textural effects of regional metamorphism on the Thunderhead Sandstone. For those portions of this study involving surface area, quartz and plagioclase alone are considered, while the mosaic study involves all major phases in the rock.

Adjustments in the rock fabric to the changing physical conditions (T, deviatoric stress) of regional metamorphism produce continual changes in the topologic network of grain boundaries and the type and orientation of phases making up the neighborhood of a given grain or aggregate of grains (5). Stressed grains repair structural damage through polygonalization-recrystallization processes (6), as well as solid-state diffusion. Stressed aggregates of grains approach textural--and metamorphic-equilibria through neighbor selection when stability limits of old neighbors have broken down (7). Additionally, large aggregates of grains may organize themselves into "super neighborhoods" through compositional banding processes (8).

PART I

GRAIN BOUNDARY TEXTURES

DISCUSSION OF THE MODEL

There are two components in the total surface area of a grain: interior, or polygonal-surface area and exterior surface area (Figure 1). These two types may be termed α-α and α-β respectively, where α-α implies that two grains of the same phase meet at a boundary, and α-β implies the junction of two different phases. These may also be termed like-like or unlike boundaries, respectively.

Our model estimates changes in both components of surface area during regional metamorphism (Figure 2). In initially unmetamorphosed sediments (left side of figure), most of the total surface area is exterior, or α-β. Only relatively minor amounts of α-α occur, and these are often diagenetically generated fractures or the chance agglutination of two grains of the same phase. Rapid increases in the α-α component occur as stored strain is relieved through polygonalization and recrystallization (6). Increases in temperature facilitate structural repair by increasing the ease of recrystallization, such that the surface area in the interior of a phase (α-α) soon comprises most of the total surface area (as illustrated by the large hump over the brittle sector).

Figure 1. Nomenclature of Surface Area Types.

definition of boundary components

UNLIKE, α-β TYPE, GRAIN–MATRIX BOUNDARIES

LIKE, α-α TYPE, SUB–BOUNDARIES

β PHASE(S) = ALL NON–α TYPE MATRIX MINERALS AND GRAINS

α PHASE = ANY PHASE WHOSE GRAIN BOUNDARY BEHAVIOR IS BEING INVESTIGATED

NOTE: β-β TYPE BOUNDARIES ARE NOT DEFINED

Figure 2. Model for changes in surface area in quartz and plagioclase, in response to the changing (P,T) conditions during regional metamorphism.

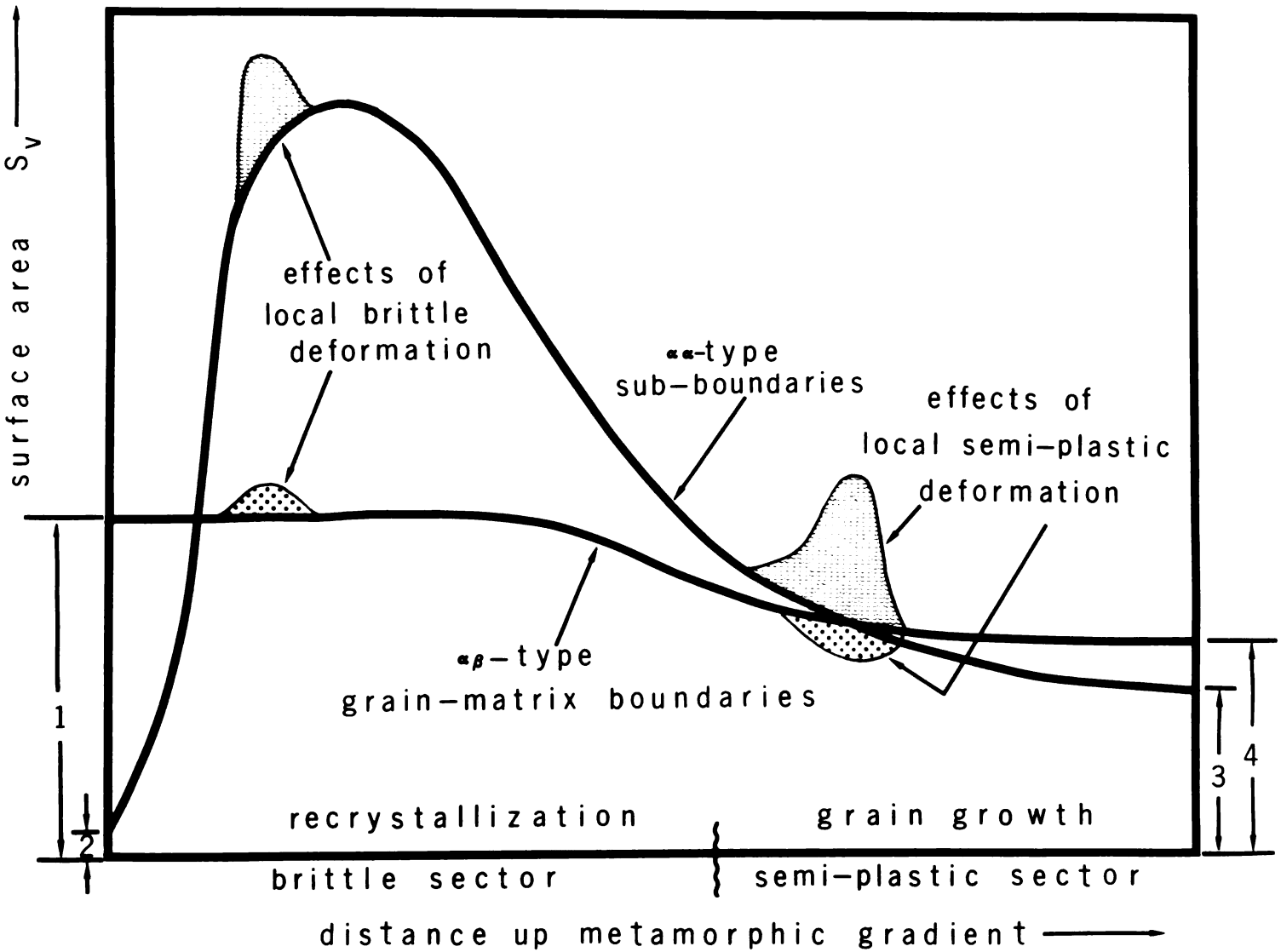
surface area S_v
effects of
local brittle
deformation
αα-type
sub-boundaries
effects of
local semi-plastic
deformation
αβ-type
grain-matrix boundaries
1
2
3
4
recrystallization
grain growth
brittle sector
semi-plastic sector
distance up metamorphic gradient

Relief of stored strain reduces the driving force producing recrystallization (6), while maintained--or increased--temperatures will aid grain growth (9). Both these effects will cause a relative reduction in like-like (α-α) boundaries. Grain growth should be expected to continue up the gradient, effecting a substantial reduction in α-α surface area through the elimination of α-α boundaries. It would be expected that the final $S_{V_{\alpha\alpha}}$ value would approach, but not equal, that in the original sedimentary fabric. Impurity levels within a phase would be expected to block some grain boundary migration (10), and therefore the elimination of subboundaries within phase interiors would not go to completion. This difference between α-α surface area in the sedimentary and equilibrium metamorphic rock is denoted $\Delta S_{V_{\alpha\alpha}}$. Exterior S_V would be expected to remain approximately constant, until the integrity of grain margins begins breakdown by like-phase agglutination in areas of semi-plastic flow. The final equilibrium S_V texture should be characterized by a relatively higher level of α-β boundaries, due to the enhanced stability of α-β margins at higher grades of metamorphism (7).

SAMPLING

Sampling within the Thunderhead Sandstone (Figure 3) was carried out at twenty-one individual sites along U.S. Route 441

Figure 3. Sketch map of the Gatlinburg, Tennessee-Cherokee, North Carolina area (after King, 1964).

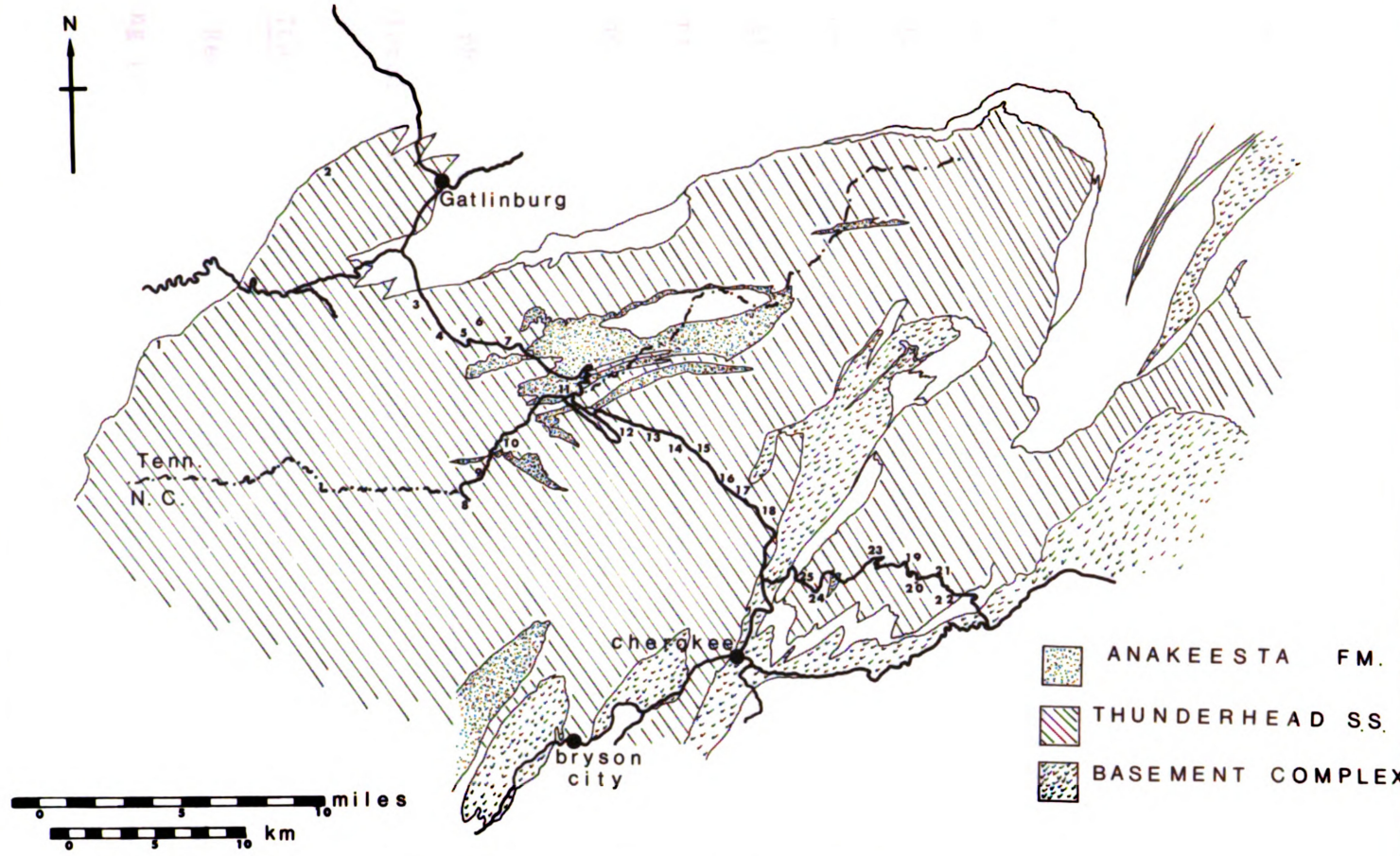

GEOLOGIC SKETCH MAP

CENTRAL GREAT SMOKY MOUNTAINS

from Gatlinburg, Tenessee to Cherokee, North Carolina. The overall direction of the sample traverse is coincident with the regional metamorphic gradient, and approximately perpendicular to all mapped isograds (Figure 4).

From the samples obtained, 36 samples were selected for textural examination. Sixteen of these were candidates for a subsequent analysis of variance which followed the preliminary examination. Samples were slabbed for thin-sectioning perpendicular to the direction of elongation of eliptical quartz grains, or the apparent foliation of the rock fabric as a whole. This provided for uniformity of orientation of each thin section with respect to the inferred regional stress field producing foliation.

Thin sections were stained for plagioclase and alkali feldspar with rhodizonic acid and sodium cobaltinitride using a procedure developed by Bailey and Stevens (11).

APPLICATION OF QUANTITATIVE STEREOLOGY

Recent developments in metallography have provided means of making three-dimensional form and structural inferences from two-dimensional microstructure (12). These metallographic approaches provide, for example, a means of abstracting volumetric surface area from observed phase boundaries in thin sections. It was therefore

Figure 4. Sketch map of the location of regional isograds (after King, 1964).

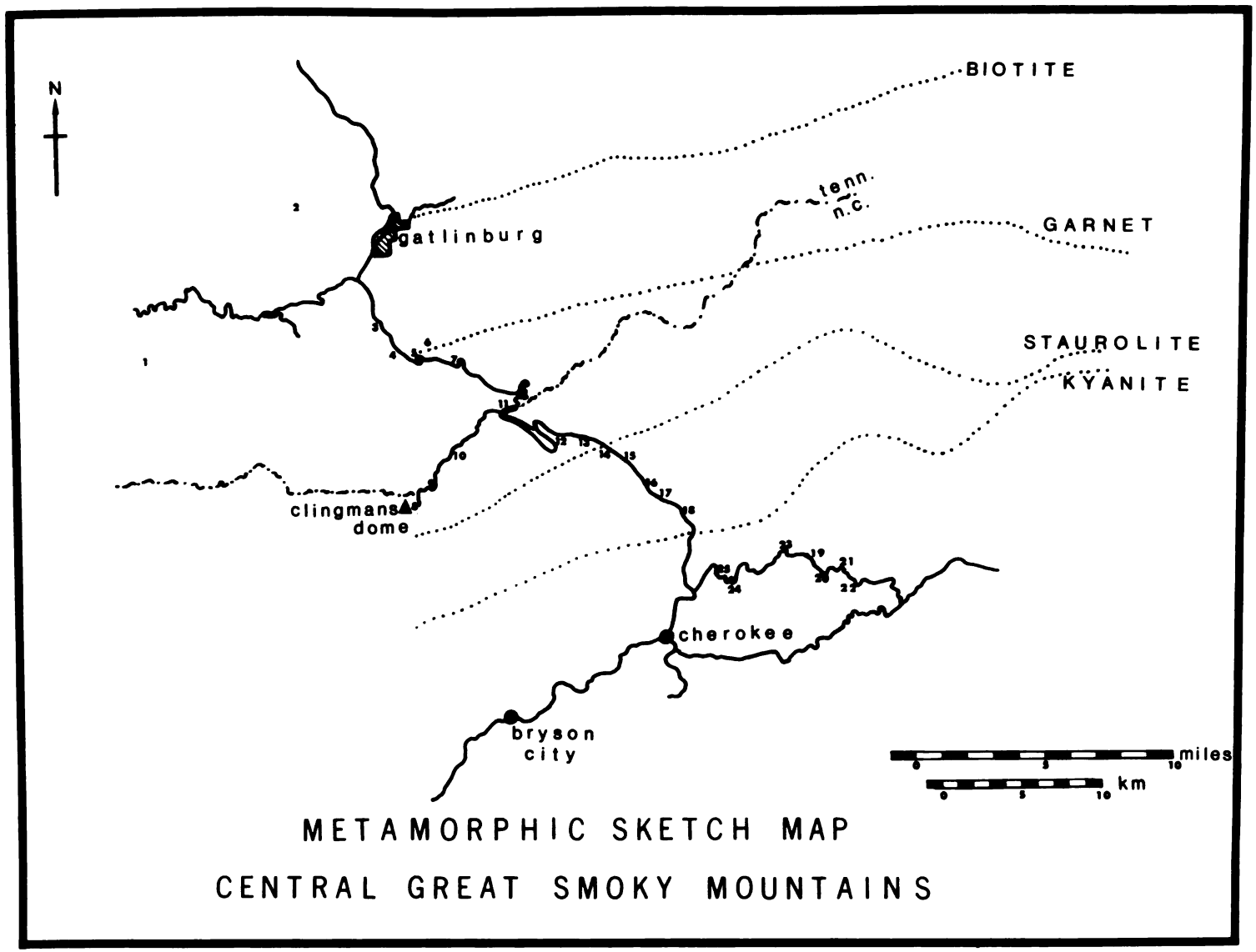

METAMORPHIC SKETCH MAP

CENTRAL GREAT SMOKY MOUNTAINS

possible to examine the extent of polygonalization and recrystallization in the quartz and plagioclase phases of the Thunderhead Sandstone, and test the recrystallization model by the application of stereologic surface area measurements.

Recrystallization of quartz and plagioclase involves energy reductions which cause adjustments in total surface area. Total surface area has an outer, or unlike phase to phase contact as well as an inner or like-like phase contact. Therefore both these boundary types must be counted in polygonalization-recrystallization studies. Subboundaries, or interior borders are α-α type contacts, while exterior, or grain-matrix margins are α-β types. Surface areas for both types of contacts are generated from the basic observation N_1, the number of intersected margins per unit line. The polygonal (interior, α-α) surface area per unit volume is given by

$$S_v = 2N_1 \qquad (1)$$

while exterior (α-β) surface area per unit volume is

$$S_v = 4N_1 \qquad (2)$$

Coefficients of 2 and 4, for expressions 1 and 2 respectively, account for both the interfacial areas at an α-α margin in the first case, and, in the second case, the fact that the outer

surficial area of the α-β margin will be counted twice since the outer surface will necessarily close upon itself. Full development of (1) and (2) may be found in Underwood (13) and DeHoff and Rhines (14). Operational determination of N_1 uses the method of random secants (13). Stained thin sections were examined on a Leitz petrographic microscope using a flat stage, 8X occular, 10X objective, and Chayes point counter. For each thin section, 30 test lines were applied. Each test line measured 1.18 mm, making a total traverse length of 35.4 mm per thin section. The position of each traverse was randomized with respect to x-y position (in the plane of the stage) under the objective, and angular orientation (θ) relative to the microscope axis. Cross hairs within the occular provided the test secant. Visual traverses were made along the test line, and α-α, α-β observations were recorded on a Swift point counter for both quartz and plagioclase; i.e., the following boundaries were counted:

1) quartz-quartz
2) quartz-others
3) plagioclase-plagioclase
4) plagioclase-others

Counts were accumulated until a total of 30 randomly-oriented traverses had been completed. Total counts were then normalized to

N_1 by division by the total cumulative traverse length. From N_1, S_v was then available by relations (1) and (2).

RESULTS

The effects of the regional metamorphic gradient on surface area in quartz and plagioclase are presented in the form of

1) plots of surface area vs. distance up the metamorphic gradient
2) the analysis of variance of surface area for selected sites
3) regression of α-α surface area onto α-β surface area
4) evaluation of the residuals from regression.

SURFACE AREA CHANGES WITH METAMORPHIC GRADE

Values of quartz-quartz, quartz-other, plagioclase-plagioclase, and plagioclase-other surface areas per unit volume (mm^2mm^{-3}) have been determined for a number of sites occupying various positions within the regional metamorphic gradient. Sample sites are identified along the absissa in Figures 5-8. The position of a site on the absissa was obtained by projecting normals from map localities onto a line perpendicular to the regional mapped isograds.

Examination of quartz-quartz S_v (open circles, Figure 5) reveals an early series of high values, which declines substantially by site 10, then undergoes a moderate rise between sites 13 to 18,

Figure 5. Variation in the surface area of quartz-quartz contacts as a function of distance up the regional metamorphic gradient.

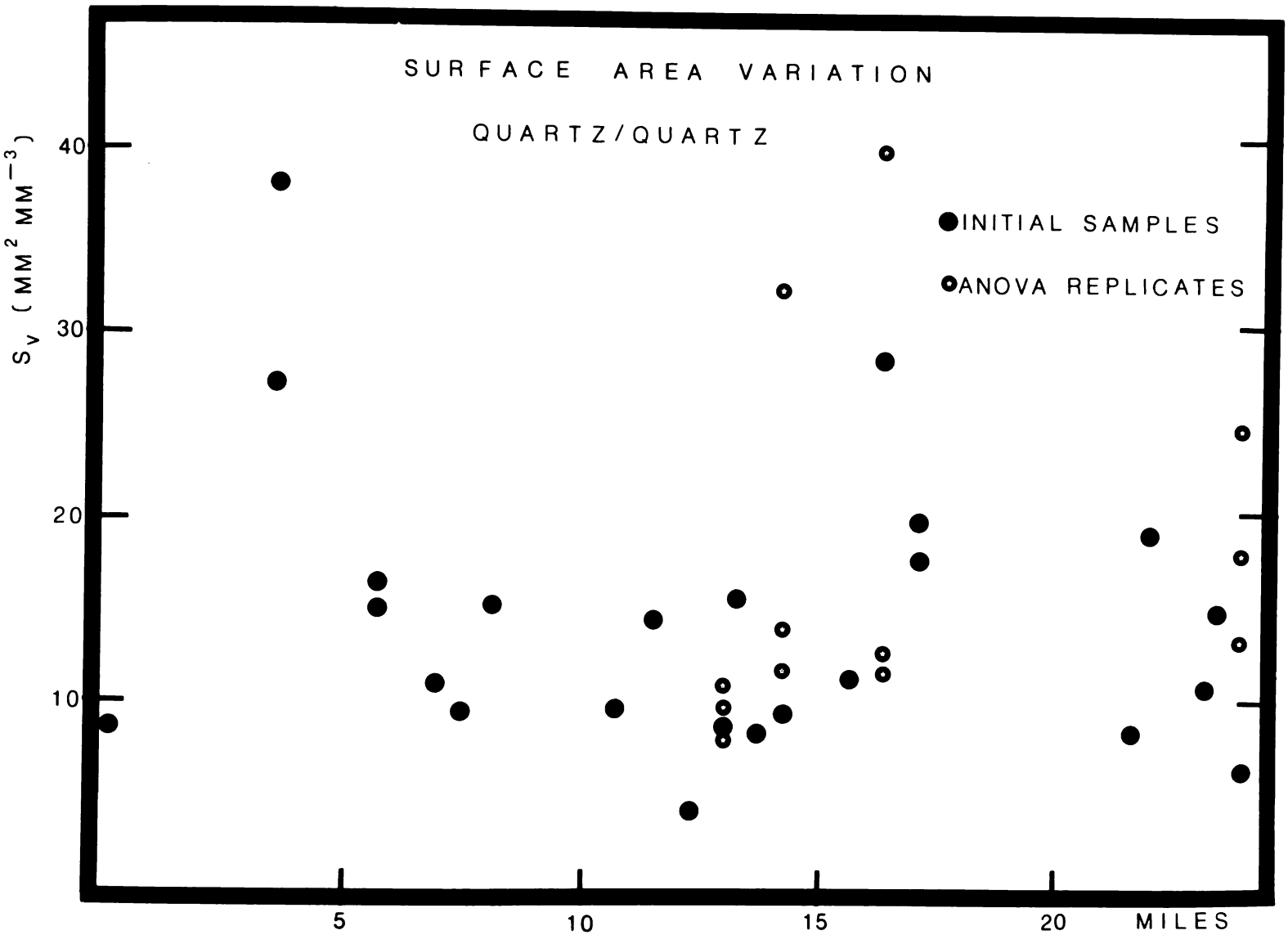
SURFACE AREA VARIATION
QUARTZ/QUARTZ
INITIAL SAMPLES
ANOVA REPLICATES
S_v (MM^2 MM^{-3})
40
30
20
10
5
10
15
20
MILES

and declines slightly by site 22. This is in general agreement with what we would anticipate with the model of Figure 2.

For quartz-other S_V (Figure 6), consideration of open-circled values shows a fairly steady series, with a slight but noticeable dip from site 8 to site 21. This is also behavior which might be expected by considering the α-β trend as outlined in the surface area model.

Variation in surface area for plagioclase-plagioclase boundaries (Figure 7) shows two rises, one centered over sample site 1 and a second centered over sample site 13.

The variation in plagioclase-other surface area (Figure 8) shows fairly steady variation about an average value near 10 mm^2mm^{-3}. A small downward movement in values, however, occurs between sites 13 and 18.

Deviation from the surface area model in plagioclase occurs in overall low α-α values and the failure of α α values to stand substantially above α-β values--especially in the early low-grade sector.

VARIANCE IN SURFACE AREA

The spread in S_V values for outcrops which received multiple testing (such as sites 1 and 2 with two values each) suggested an evaluation of the variance in surface area at selected sites.

Figure 6. Variation in the surface area of quartz-other contacts as a function of distance up the regional metamorphic gradient.

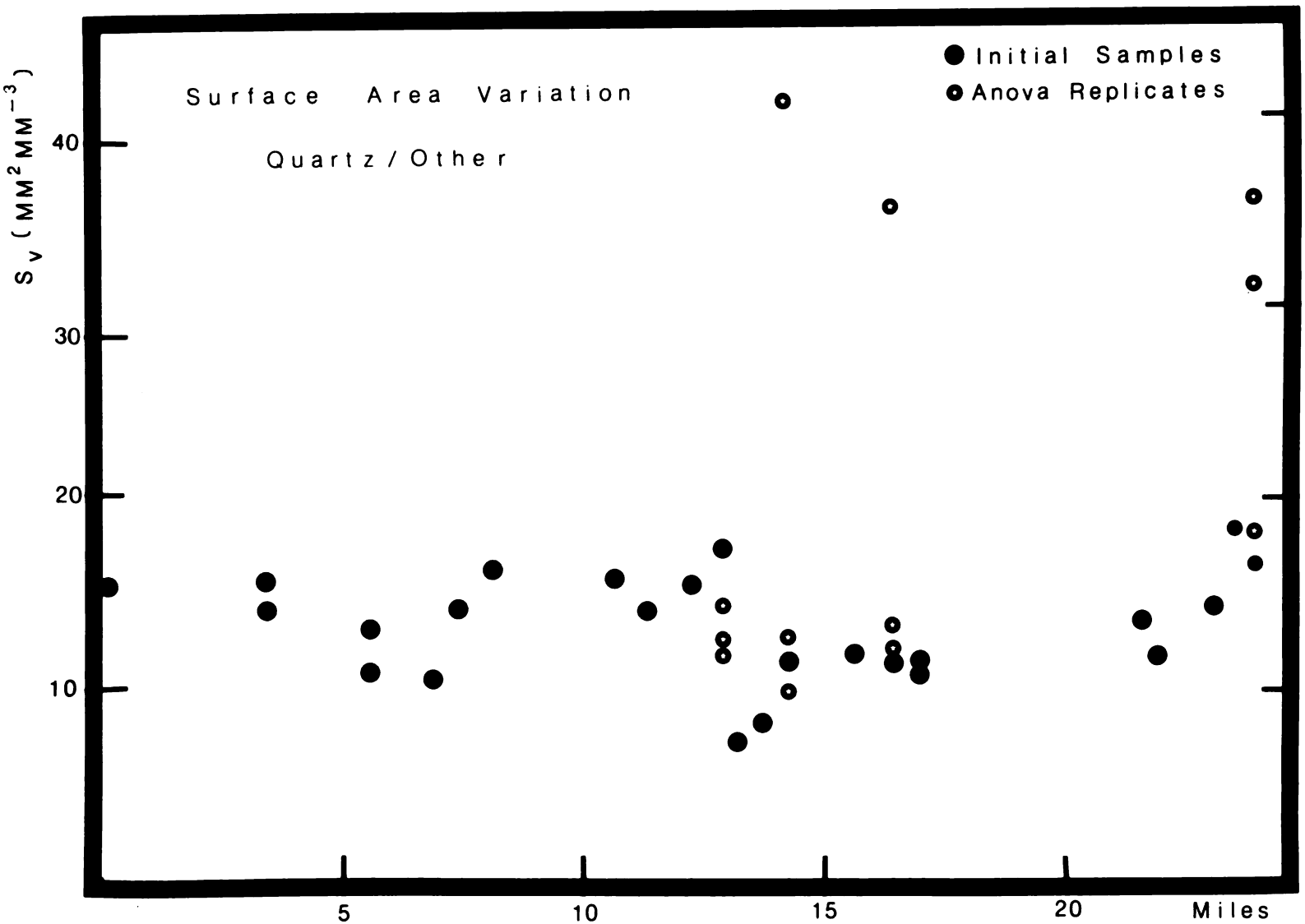
Surface Area Variation
Quartz / Other
Initial Samples
Anova Replicates
S_v ($MM^2 MM^{-3}$)
40
30
20
10
5
10
15
20
Miles

Figure 7. Variation in the surface area of plagioclase-plagioclase contacts as a function of distance up the regional metamorphic gradient.

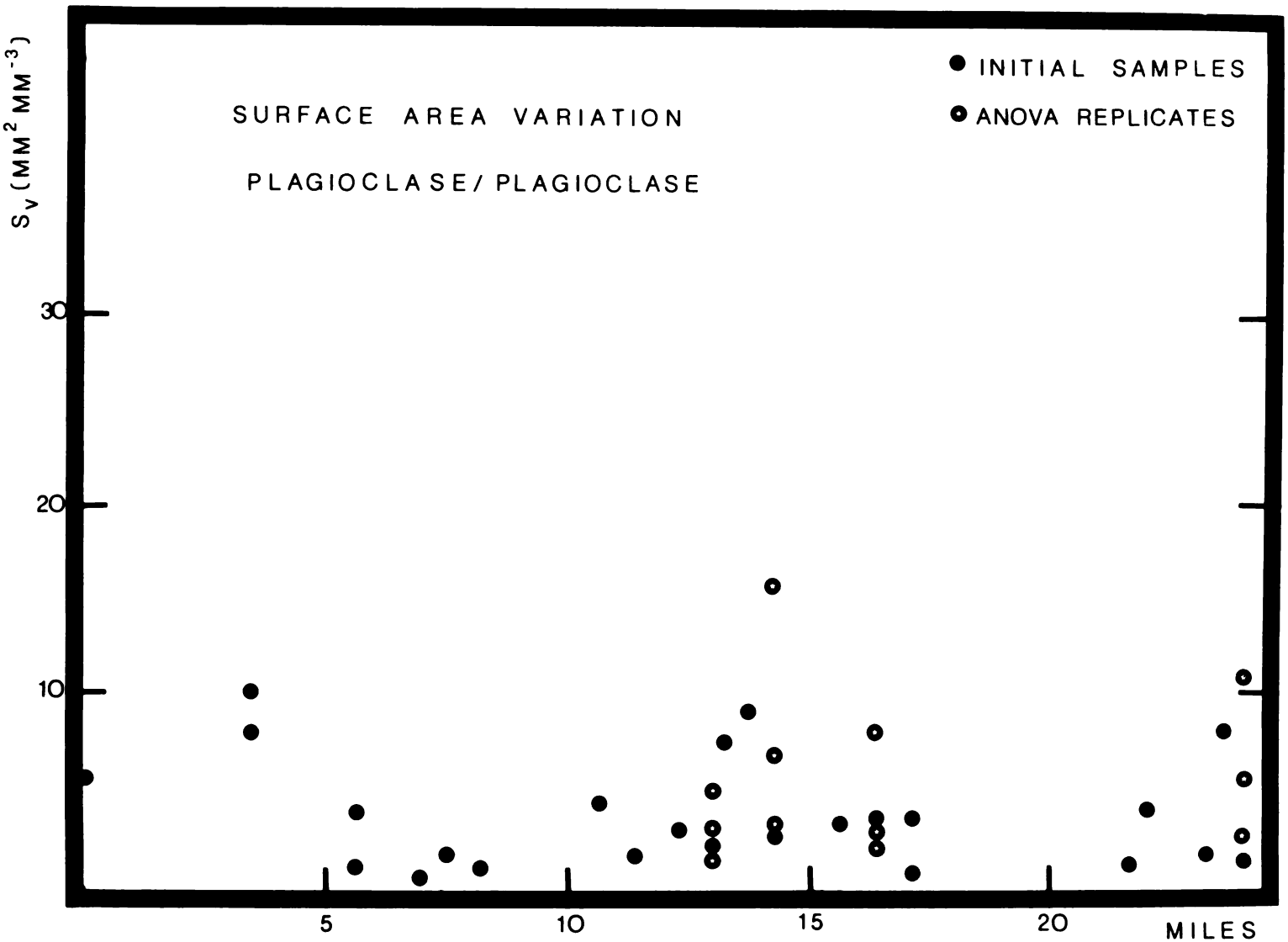
SURFACE AREA VARIATION
PLAGIOCLASE/ PLAGIOCLASE
INITIAL SAMPLES
ANOVA REPLICATES
S_v (MM^2 MM^{-3})
30
20
10
5
10
15
20
MILES

Figure 8. Variation in the surface area of plagioclase-other contacts as a function of distance up the regional metamorphic gradient.

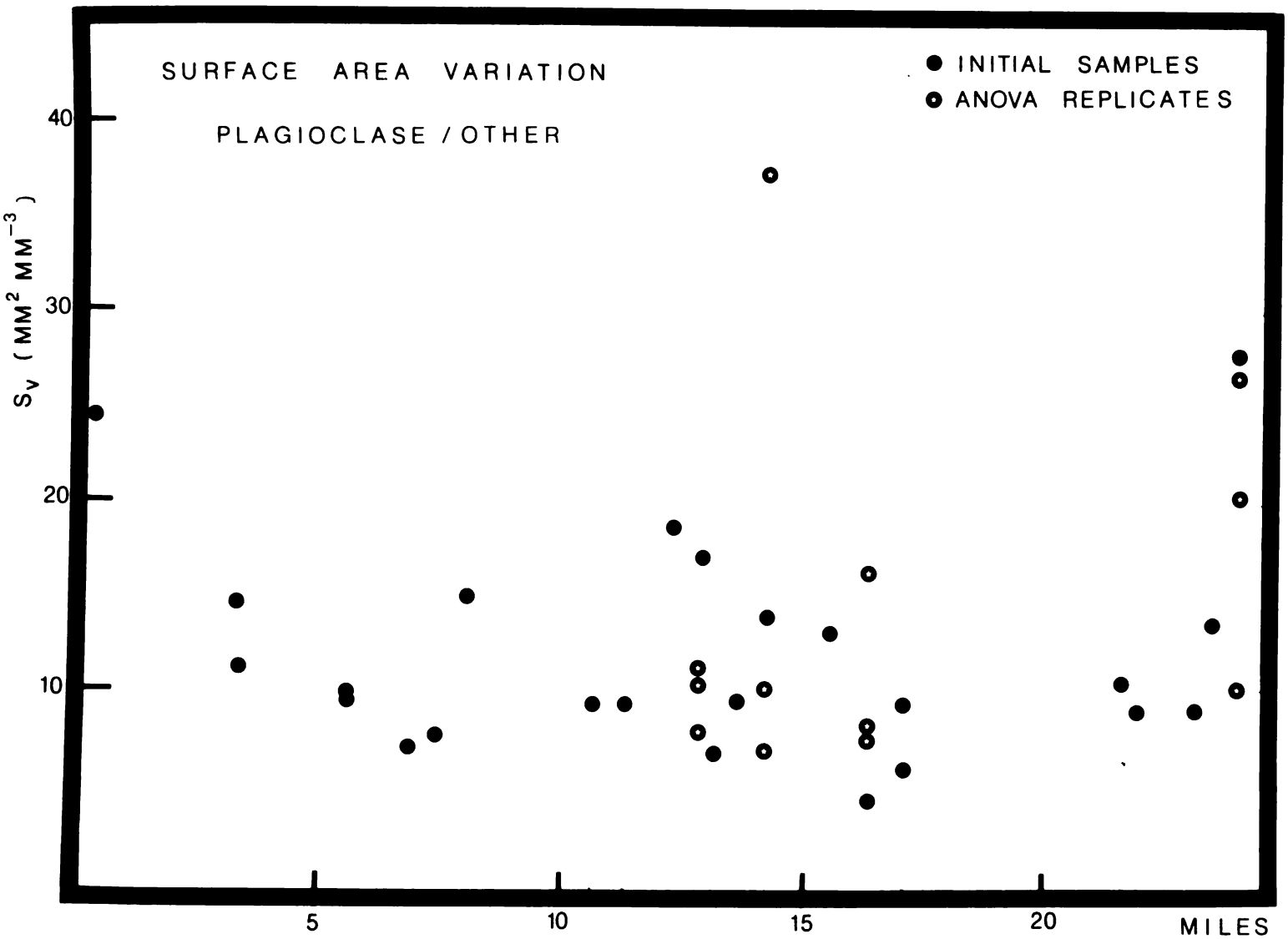
SURFACE AREA VARIATION
PLAGIOCLASE / OTHER
INITIAL SAMPLES
ANOVA REPLICATES
S_V (MM^2 MM^{-3})
40
30
20
10
5
10
15
20
MILES

Meaningful evaluation of changes in S_V over the metamorphic gradient are critically dependent on a knowledge of the extent of variation within an outcrop or sample site.

From the total spread of sample sites, four sites were chosen at random for the analysis of variance. From available samples for each site (generally 10 to 15), four samples were randomly selected for subsequent thin sectioning and surface area measurements by methods described earlier. Those samples involved in the analysis of variance are represented by black dots above their sample sites on Figures 5 to 8.

The analysis of variance decomposes the total variance (all samples at all sites) into a component within the sample site and a component between the sample sites. The magnitude of the difference between these two components is determined through the F test statistic. The null hypothesis (H_o) states that the values of S_V from all samples at all sites, come from the same population. The alternate hypothesis (H_i) states that S_V values from different sample sites come from different populations. Rejection of the null hypothesis at a given level of significance requires exceeding corresponding tabled values of F. Details of the computational steps and complete discussions of analysis of variance are given by Sokal and Rohlf (1969) and Griffiths (1967).

Results of the analysis of variance α-α, α-β S_v in quartz and plagioclase are presented in Tables 1 through 4. These evaluate the components of variance for sample sites 8, 15, 17 and 22. This is a range of 12 miles on the metamorphic gradient, although representation of the entire gradient was assured through the process of random selection. Rejection of the null hypothesis at an α-level of .05 requires an F statistic value of 3.49 or greater. In no instance was this value met, and the null hypothesis has failed to be rejected. We conclude, therefore, that from the sample sites selected to represent the metamorphic gradient, there are sites which contain as much variation within themselves as between sites over the gradient as a whole.

TABLE 1: SITES 8, 15, 17, 22

Analysis of variance: Quartz-Quartz S_v

Source	df.	ss	MS	F
Among sites	3	370.216	123.405	1.47
within sites	12	1001.353	83.446	
Total	15	1371.569		

TABLE 2: SITES 8, 15, 17, 22

Analysis of variance: Quartz-others S_v

Source	df.	ss	MS	F
Among sites	3	274.912	91.637	0.804
within sites	12	1366.540	113.878	
Total	15	1641.452		

TABLE 3: SITES 8, 15, 17, 22

Analysis of variance: Plagioclase-Plagioclase S_v

Source	df.	ss	MS	F
Among sites	3	35.502	11.834	0.745
within sites	12	190.481	15.873	
Total	15	225.983		

TABLE 4: SITES 8, 15, 17, 22

Analysis of variance: Plagioclase-other S_v

Source	df.	ss	MS	F
Among sites	3	344.211	114.737	1.601
within sites	12	859.851	71.654	
Total	15	1204.062		

The 4 site-16 sample analyses were broken down into a number of smaller analyses involving two sample sites. Results of these breakdowns are presented in Tables 5 through 9. Reduction in the number of sites changes the degrees of freedom for both the "among sites" and the "within sites" sources of variation. This requires comparison of the calculated F statistic with new tabulated values. Rejection of the null hypothesis now requires an F value of 5.99 for significance at the 95% level, and 13.7 for an α-level of .01.

TABLE 5: SITES 8, 17

Analysis of variance: Quartz-Quartz S_v

Source	df.	ss	MS	F
Among sites	1	368.833	368.833	4.108
within sites	6	538.694	89.782	
Total	7			

TABLE 6: SITES 8, 17

Analysis of variance: Quartz-Others S_v

Source	df.	ss	MS	F
Among sites	1	33.620	33.620	0.471
within sites	6	427.392	71.232	
Total	7	461.012		

TABLE 7: SITES 8, 22

Analysis of variance: Quartz-Others S_v

Source	df.	ss	MS	F
Among sites	1	266.805	266.805	5.509
within sites	6	290.573	48.428	
Total	7			

TABLE 8: SITES 8, 15

Analysis of variance: Plagioclase-Plagioclase S_v

Source	df.	ss	MS	F
Among sites	1	125.091	125.091	33.50
within sites	6	22.404	3.734	
Total	7			

TABLE 9: SITES 17,22

Analysis of variance: Plagioclase-Others S_v

Source	df.	ss	MS	F
Among sites	1	286.084	286.084	6.398
within sites	6	268.284	44.714	
Total	7	554.368		

Highly significant rejection of H_o (α = .005) for plagioclase-plagioclase S_v at sites 8 and 15 (Table 8) shows that differences in the relative amounts of recrystallization and grain growth are present.

Significant rejection of H_o (α = .05) for plagioclase-others S_v between sites 17 and 22 (Table 9) show that differences in the outer component of S_v (α-β) are present. In the surface area model, these sites correspond to points in the higher-grade rocks where semi-plastic behaviour should become increasingly important. Hence, semi-plastic agglutination of plagioclase between sites 17 and 22 may explain the substantial reduction in S_v.

REGRESSION

The regression of α-α S_v on α-β S_v for quartz is shown in Figure 9. Values of the simple correlation coefficient (ρ), and the multiple correlation coefficient (R^2) are 0.5339 and 0.2851 respectively. In the analysis of variance for overall regression, the slope β_1, (here β_1 is an estimator for the parametric slope b_1, and should not be confused with a β phase or grain boundary) of 0.5741 was significant at the 99.9% level.

The regression line divides the graph into two fields. Strong deviation from regression in field I indicates samples that have the great bulk of their total S_v taken up by α-α subboundaries

Figure 9. Grain boundary diagram, showing the amount of total surface area in quartz which is allocated to subboundaries (quartz-quartz) and to neighbor boundaries (quartz-other). A diagonal from the origin would divide this into two fields: upper field suggests large amount of recrystallization; lower field suggests granulation trend.

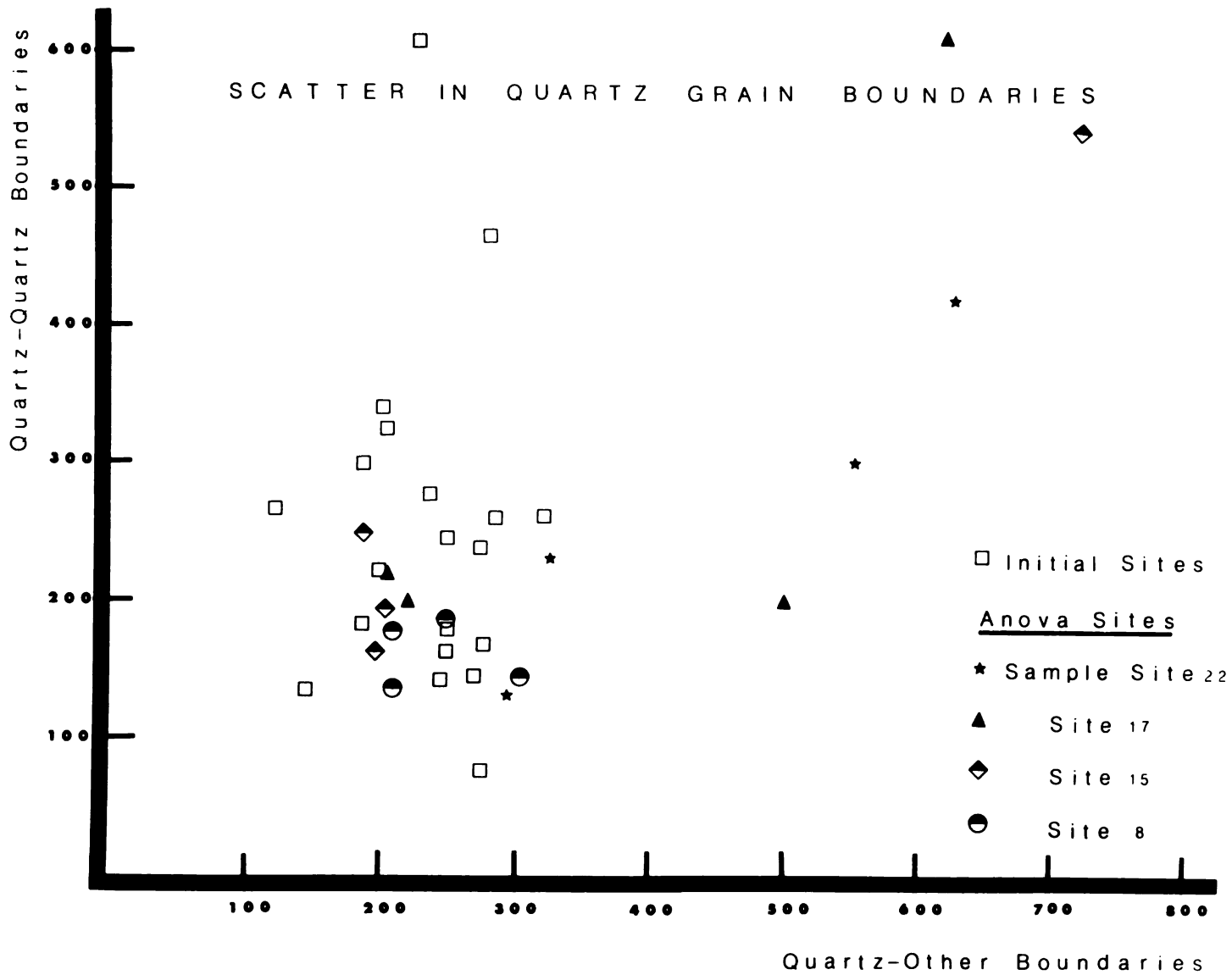
SCATTER IN QUARTZ GRAIN BOUNDARIES
Quartz-Quartz Boundaries
600
500
400
300
200
100
100
200
300
400
500
600
700
800
Quartz-Other Boundaries
Initial Sites
Anova Sites
Sample Site 22
Site 17
Site 15
Site 8

(1-13-A and 1-10-b). These occupy the α-α peak in the surface area model. Samples deviating strongly form regression in field II have relatively few α-α boundaries, and most of the total S_V is exterior (sample 17-2).

Samples involved in the S_V analysis of variance are indicated by geometric shapes. Substantial scatter in values for a single outcrop site (Figure 9) is shown in plots for site 17 (triangles) and site 22 (circles). At site 17, separation of 17-2 form the main cluster indicates that recrystallization has been relatively surpressed. Very large α-α S_V and α-β S_V values for sample 17-4 indicates a large relative increase in both recrystallization and dispersion of the quartz phase. This difference in S_V behavior between 17-4 and the 17-1, 17-3 cluster may not be explained by differences in quartz content (samples 17-4, and 17-1 contain 42.75% and 46.75% quartz respectively).

Marked scatter also occurs in plots of the S_V components for samples from site 22. In this case there is an approximately linear range of (α-α S_V, α-β S_V) values for the series 22-2A, 22-4, 22-5 and 22-6. The range in modal % quartz for these samples is 45.75 to 49.50--a separation of less than 5%. Explanation for such large differences in recrystallization within one sample site may lie in proximity to pelitic interbeds, and/or point-to-point differences in

deviatoric stress. At site 17, for example, samples 17-1, 17-3 were relatively removed from pelitic layers, while 17-2 and 17-4 were quite close. Sample 17-4 was the closest of all, being one foot below a two-foot-thick pelitic layer.

For the regression of α-α on α-β S_V in plagioclase (Figure 10), analysis of variance for overall regression shows $\beta_1 = 0.2615$ at the 99.9% level of significance.

For plagioclase S_V, as in quartz S_V, site 1 shows strong deviation from regression (in field I) indicating high levels of recrystallization. Samples from site 22 (circles) show scatter in their plots. The plagioclase content of these rocks varies from 22.25% to 30.25%. The variance in modal % is small (8%) and does not have a systematic relationship with S_V. The explanation for scatter in S_V within a single outcrop appears to lie outside the variation in modal % (as in quartz).

For quartz-quartz S_V at sites 8 and 17 (Table 5), standards must be reduced to a 90% significance level for rejection of H_o. For quartz-quartz S_V variation among all four sample sites considered in the original analysis of variance (Table 1), the most significant differences (from a consideration of Figure 5) appear to be between sites 8 and 17. The failure to reject H_o at the 95% level of significance, however, indicates that substantial difficulties may

Figure 10. Grain boundary diagram for plagioclase. See Figure 9 caption also.

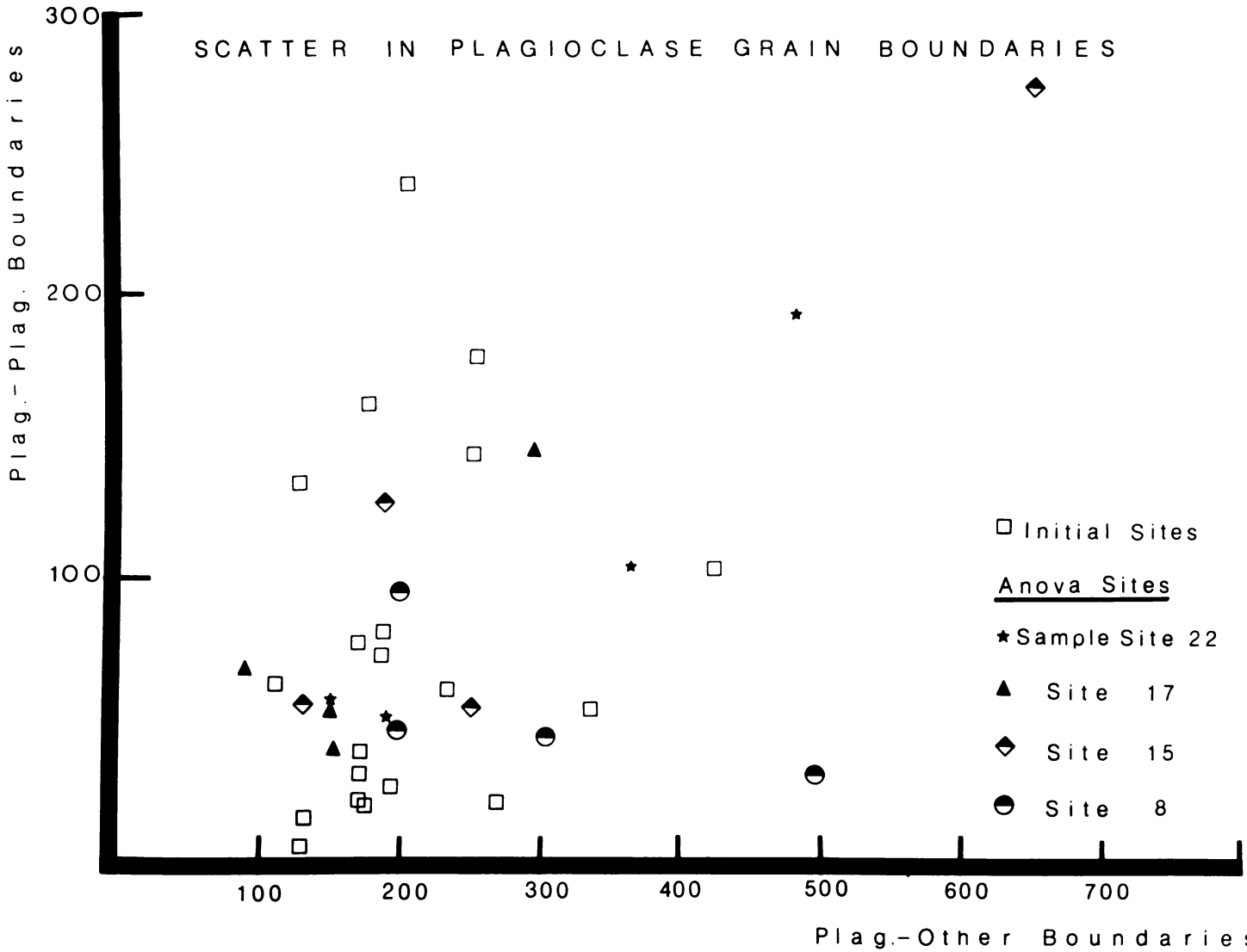
SCATTER IN PLAGIOCLASE GRAIN BOUNDARIES
Plag.-Plag. Boundaries
300
200
100
100
200
300
400
500
600
700
Plag.-Other Boundaries
Initial Sites
Anova Sites
Sample Site 22
Site 17
Site 15
Site 8

lie in the way of using quartz S_v as an estimator of position on the regional metamorphic gradient. Similar variations in quartz S_v with metamorphic grade were found in the Cross Lake Pluton in an earlier textural study.

RESIDUALS FROM REGRESSION

Figures 11 and 12 plot the deviations of individual observations from regressing α-α S_v on α-β S_v for quartz and plagioclase respectively. These residuals are plotted over the positions their sample sites occupy on the metamorphic gradient. The upper portion of each figure contains samples which have a predominance of α-α -type S_v. The lower portion contains those samples which have the larger portion of their total S_v tied up in the outer, or α-β component. Plotting residuals in this manner permits an evaluation of trends in the variance of S_v up the metamorphic gradient as well as an examination of the goodness of fit to the assumptions of least-square regression (18).

Both Figures 11 and 12 show a non-random behavior of S_v variance in the distance sequence plot. For both quartz and plagioclase, variance from regression decreases from early large positive values (site 1) through zero to large negative values near sites 7-11. Both quartz and plagioclase show subsequent reductions in negative variance through zero to sizable positive variances. This second "high" is centered on site 17 for quartz and on sites 13-15 for plagioclase.

Figure 11. (Non-random) distribution of the residuals from regression for all quartz boundary types.

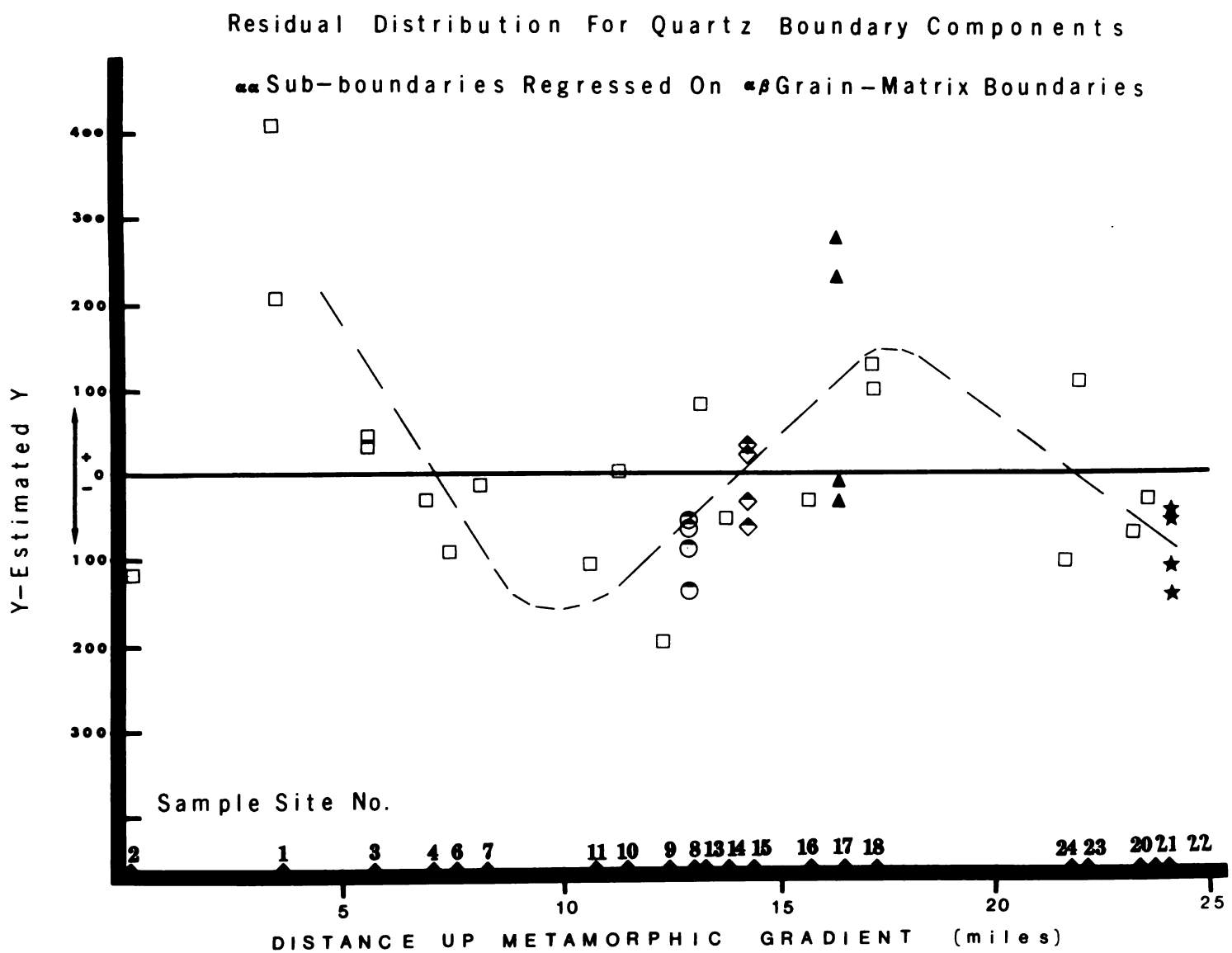
Residual Distribution For Quartz Boundary Components
αα Sub-boundaries Regressed On αβ Grain-Matrix Boundaries
Y-Estimated Y
400
300
200
100
+
-
0
100
200
300
Sample Site No.
2 1 3 4 6 7 11 10 9 8 13 14 15 16 17 18 24 23 20 21 22
5
10
15
20
25
DISTANCE UP METAMORPHIC GRADIENT (miles)

Figure 12. Distribution of the residuals from regression for plagioclase boundary types.

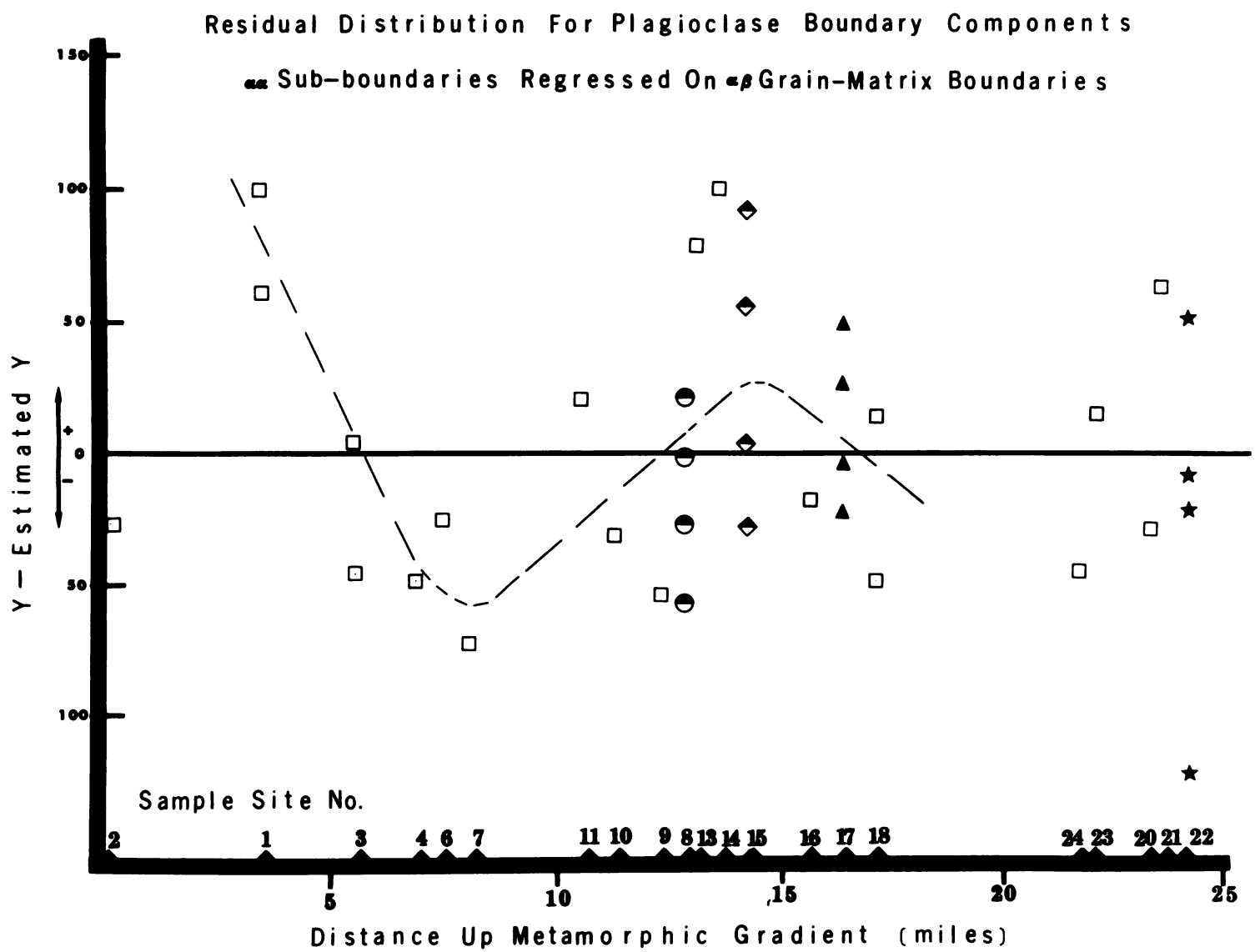
Residual Distribution For Plagioclase Boundary Components
αα Sub-boundaries Regressed On αβ Grain-Matrix Boundaries
Y — Estimated Y
150
100
50
+
0
-
50
100
Sample Site No.
2 1 3 4 6 7 11 10 9 8 13 14 15 16 17 18 24 23 20 21 22
5
10
15
20
25
Distance Up Metamorphic Gradient (miles)

In the case of quartz, a final decline through zero to negative values occurs between sites 18-22. Variance in plagioclase appears to tail off and distribute itself widely about the zero line. In general, rises and declines in variance for quartz are fairly tightly grouped, while those for plagioclase show more spread.

If distance up the metamorphic gradient had no effect on the regression data, we should expect a fairly horizontal band of residual plots. This band would be centered about the zero-deviation line. The sinuous variation in deviations for quartz and plagioclase, (dashed line in Figures 11 and 12) plus the apparent synchronous rise and fall of these deviations indicates that the ratio of α-α to α-β surface area is highly dependent on position within the gradient. This is what one might expect from consideration of the surface area model (Figure 2), as the model essentially tries to anticipate changes in the ratio of α-α S_v to α-β S_v with distance. The second group of large positive values in Figures 11 and 12 show a relative increase in importance of α-α subboundaries from sites 7-11 to sites 13-17. This implies a second location of high amounts of recrystallization. This second "high" coincides with the location where the Greenbrier Fault system intersects the sample traverse (19).

The effects of local deformation in those sectors of the gradient where we should expect brittle or semi-plastic response are

shown in Figure 2. Cross-hatched areas indicate the effect on the α-α and α-β components of S_v.

The distributions of the residuals from regression are shown in Figure 13. Quartz residuals show clear non-normal distribution and are skewed to the right. Plagioclase residuals are approximately normally distributed.

Two assumptions of least-square regression are normal distribution of residuals about the zero deviation line, and horizontal banding of the residual plots. In quartz, both assumptions have been violated, while in plagioclase only the horizontal distribution condition is not met.

Failure of the residuals to meet the assumptions of least-square regression indicates that the components of S_v in quartz and plagioclase do not have a purely linear variation with metamorphic grade. Instead, the components of S_v show sinusoidal variation up the metamorphic gradient.

Figure 13. Residual distribution for quartz and plagioclase.

DISTRIBUTION OF REGRESSION RESIDUALS FOR $S_{V_{\alpha\alpha}}, S_{V_{\alpha\beta}}$

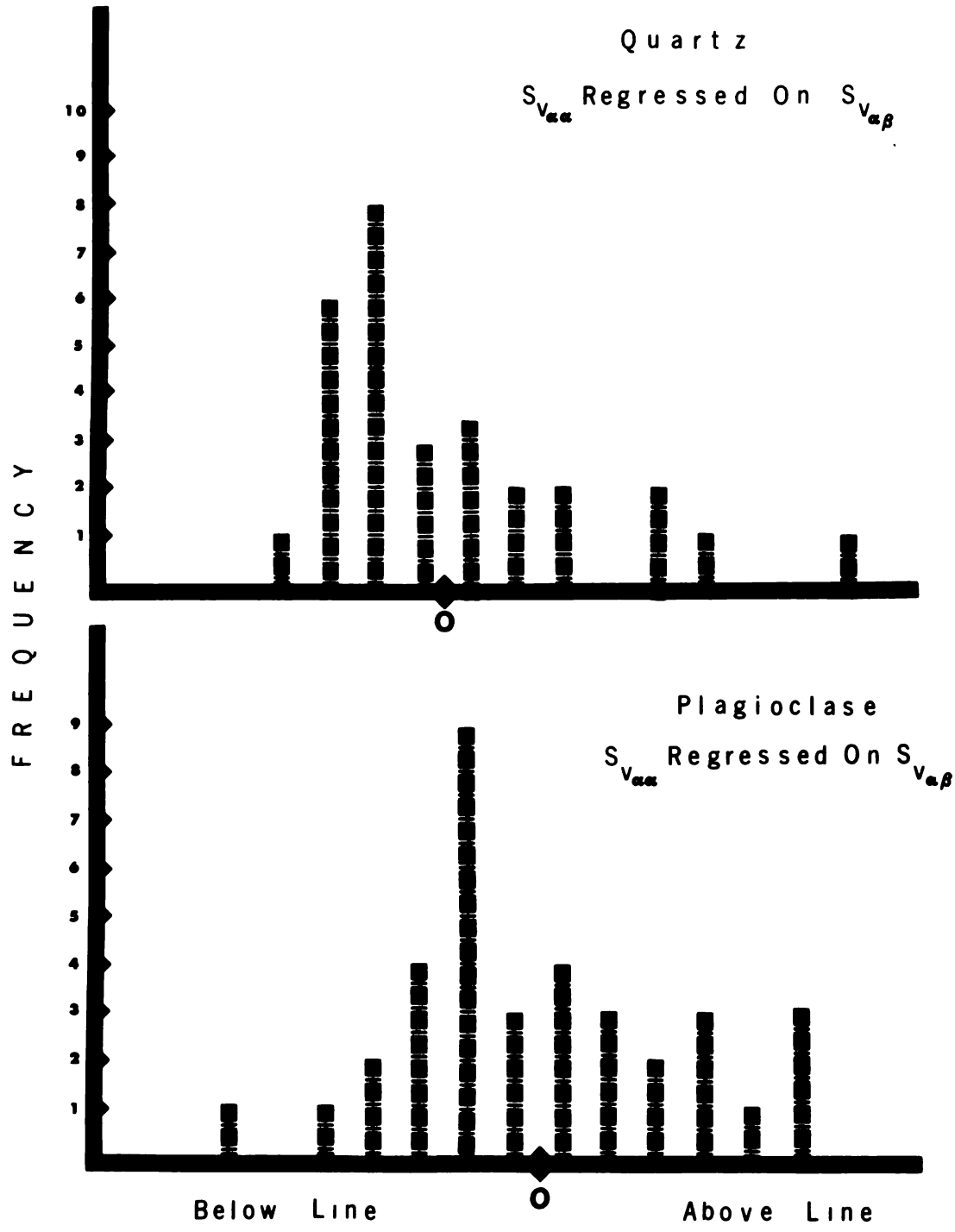

PART II

GRAIN AGGREGATE TEXTURES

MOSAIC PATTERNS AND GRAIN AGGREGATE TEXTURAL CHANGES

In this section, textural changes developed in the rock fabric are modeled in terms of mosaic pattern changes to regional metamorphism. These changes involve aggregates of grains and their changing associations with neighbors as the physical conditions (P, T) of metamorphism change. The general textural model is therefore extended to include neighborhood changes and their expected effect on the textural mosaic. The mosaic model is tested by making estimations of the amount of Markov character present in the phase aggregations.

TEXTURAL MOSAICS

The imposition of the changing P, T, and deviatoric stress components of a regional metamoprhic gradient upon sedimentary rock fabrics will induce textural disequilibria. Readjustments to equilibrium by changes in surface area have been discussed in a former section. This section will examine those textural changes which alter the phase mosaic.

For grain aggregates, readjustment to textural equilibrium involves the orientation of phases into directions of preferred

growth, until compositional layering is produced in directions perpendicular to the greatest local principal stress component (8). Such an ordering should produce neighborhood mosaics with rythmic phase repetitions, also in directions coincident with the differential stress. The end stage of such a mosaic model would be a banded rock fabric.

It should therefore be possible to examine the effects of regional metamorphism on the Thunderhead Sandstone by comparing the textures of sampled rocks with the metamorphic mosaic model.

TESTING THE MOSAIC MODEL

The sequences of mineral phases generated by traverses across rock fabrics may be conceived of as states in a Markov process. Such conceptualization provides a means of quantitatively estimating the strength of association between aggregations of phases within the rock fabric. Vistelius (20) and Kretz (21) have domonstrated the utility and power of Markov approaches to rock textural evaluation.

In a first-order Markov process, the state currently occupied influences the nature of the next succeeding state. Passage from state to state is termed a transition, and knowledge of the total variation in the composition of states, and their relative proportions, permits probabilistic statements to be made about transitions, providing the identity of the initial, or starting state, is known.

The evaluation of modal variations within the Thunderhead Sandstone permitted assignments of Mineral phases to states in the Markov process. Two coding formats were used, and the results of each format compared. The initial scheme followed the code:

1 = quartz

2 = plagioclase

3 = others

State 3, "others" consisted of mica, alkali feldspar plus very small amounts of incidental opaques and calcite. A second code lumped plagioclase and alkali feldspar together, and the new format was

1 = quartz

2 = feldspar

3 = others

where "others" were now almost totally micas.

The coded states and their transition probabilities may be viewed schematically (Figure 14, below) (22).

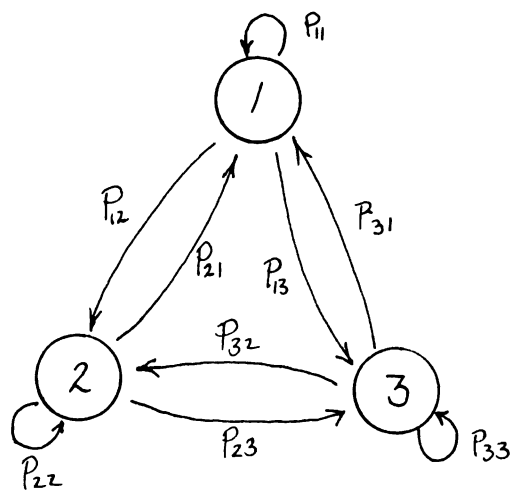

P_{ij} is the assigned transition probability of passage from state i to state j. In the case of i = 1, j = 2, P_{ij} is the probability of passage from a quartz to a feldspar observation under coding format 2. When i = j, P_{ij} becomes the likelihood of a phase observation succeeding itself, e.g., a mica observation followed by another mica observation.

Observed transitions are compiled in the form of a transition frequency matrix. For both coding formats, the three states form the 3x3 matrix:

$$\begin{array}{c} \\ 1 \\ 2 \\ 3 \end{array} \begin{array}{c} \begin{array}{ccc} 1 & 2 & 3 \end{array} \\ \begin{pmatrix} N_{11} & N_{12} & N_{13} \\ N_{21} & N_{22} & N_{23} \\ N_{31} & N_{32} & N_{33} \end{pmatrix} \end{array}$$

where 1, 2, 3 are coded states and the n_{ij}'s are the total observed phase-phase transitions (23).

The transition probability matrix is formed by row-summing the transition frequency matrix, and dividing each frequency element by its row sum:

$$[P] = \begin{array}{c} \\ 1 \\ 2 \\ 3 \end{array} \begin{array}{c} \begin{array}{ccc} 1 & 2 & 3 \end{array} \\ \begin{pmatrix} P_{ij} & . & . \\ . & . & . \\ . & . & . \end{pmatrix} \end{array} .$$

All rows will now sum to 1, since states must succeed each other. Testing for Markov character follows the method of Anderson and Goodman (24). The null hypothesis states that events (in this case phases) are independently distributed. Rejection of H_o in favor of the alternate establishes Markov character. The computational form of the test statistic is

$$-2 \text{ Log}_e \lambda = \sum_{ij} N_{ij} \text{ Ln } (\frac{P_{ij}}{P_j})$$

where n_{ij} are observed transition frequencies; P_{ij} is the transition probability from the ij'th cell; and P_j are marginal probabilities from the j'th column, formed by column totaling the transition frequency matrix, and dividing by the grand total:

$$P_j = \sum_{i}^{n} N_{ij} \; / \; \sum_{ij}^{n} N_{ij} \; .$$

The test statistic is distributed as X^2 with $(n-1)^2$ degrees of freedom. The relative magnitude of $-2\log_e \lambda$ provides a measure of the strength of association of the coded phases, and is therefore a measure of the amount of textural determinism in the Thunderhead Sandstone rock fabric. This should hence monitor the neighborhood changes wrought by regional metamorphism.

METHOD

Samples selected were the same as those chosen for the earlier surface area studies. Slabbing for thin section preparation was done

in a plane perpendicular to the maximal lineation in mineral phases, and foliation in the rock fabric. Therefore the planes of examination contained the intermediate elliptical (x-y) axes of distended mineral phases, as opposed to the maximum (z) axes of elongation (see Figure 15 below).

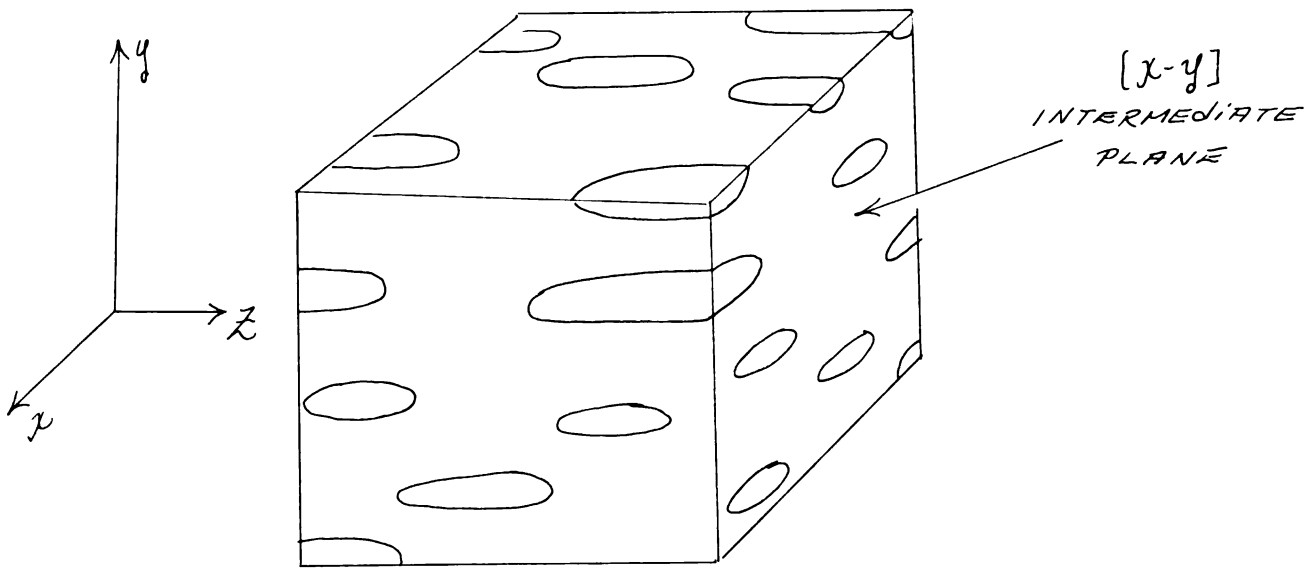

Since in nearly all fabrics, varying amounts of anisotropy were present, each fabric sample was examined in two primary directions, one perpendicular and the other parallel to lineation. A similar approach was taken by Pielou (25) who examined vegetation mosaics developed under conditions of strong prevailing wind. In each thin section, the position of maximum anisotropy was determined by construction of a series of Rose orientation diagrams (Figure 16). Unit-length traverses were made of the rock fabric on 15° intervals. At each interval, observations of intersected quartz-matrix and

Figure 16. Rose diagrams for development of anisotropy in rock texture.

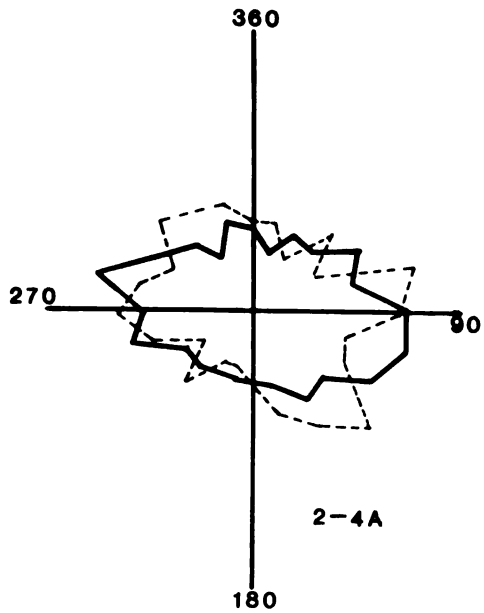

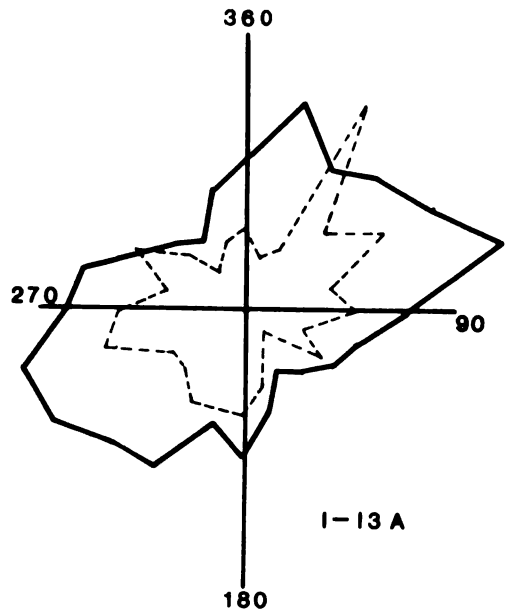

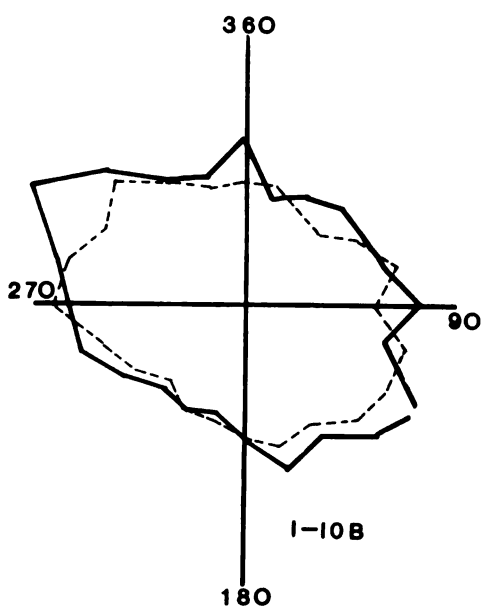

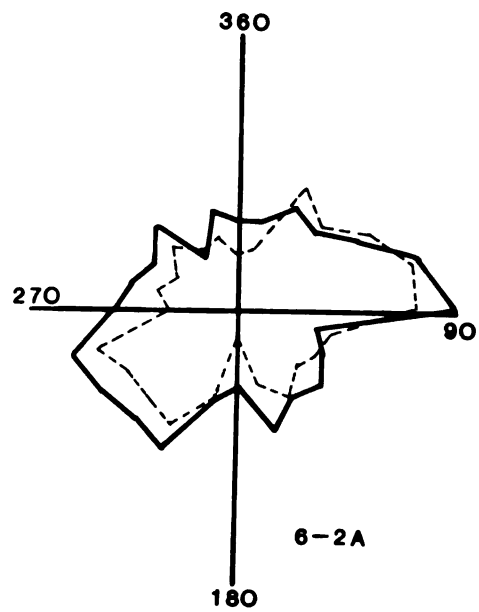

POLAR PROJECTIONS OF ROCK FABRIC TRENDS

plagioclase-matrix grain boundaries were recorded. These observations were then plotted on polar graph paper to construct the fabric Rose (13). Directions of maximal and minimal anisotropy are loci of minimal and maximal peak modes, respectively.

For each rose diagram, two angles are determined that relate the orientation of fabric anisotropy to the Chayes point counter affixed to the microscope stage. One angle relates the direction perpendicular to fabric anisotropy with the microscope axis, and the other relates the direction parallel to detected anisotropy to the axis. These angles are θ and θ_{11}, respectively. It is therefore possible to mount the rock thin section in the counter and turn the stage through some angle θ which will position the rock fabric for traverses perpendicular or parallel to the anisotropy as identified by the roses. The traversing of thin sections was performed on a Leitz petrographic microscope, using a 16 power objective and 3.5 occular. Trials with various combinations of occulars and objectives were performed, until a match was found which provided minimal redundancy (several cross-hairs falling in the same phase), and maximized the amount of total observed variation without loss of information (periodicity of phase changes shorter than cross-hair spacing).

For each θ value, as determined by the rose diagrams, 25 traverses were performed. The starting position of each traverse

was randomized with respect to the x-y plane of the thin section, however each traverse in a group of 25 was performed parallel to the orientation angle θ. All traverses started on the left cross-hair and ended on the right. For each traverse, the phase intersected by the cross-hair was noted and recorded. The eleven observations per traverse formed a chain of ten transitions. Each thin section would therefore be tested by 275 data points in each of the two cardinal rock fabric directions. This generated 250 transitions perpendicular to the direction of lineation and 250 transitions parallel to the direction of lineation. Phase observation data points from each traverse were key punched into data cards. These cards were then evaluated by a modified Fortran routine of Harbaugh and Bonham-Carter (26), which formed transition frequency and transition probability matrices. Matrices so formed were further tested for Markov character by calculation of $-2\log_e \lambda$ on a desk calculator.

RESULTS

Non-Collapsed Chains

For perpendicular-to-fabric traverses, values of $-2\log_e \lambda$ vs. distance up metamorphic grade are plotted in Figure 17. Dotted horizontal lines indicate the α-levels for rejection of the null hypothesis of independence of association among the phases quartz,

Figure 17. Degree of determinism in texture as a function of distance up the regional gradient.

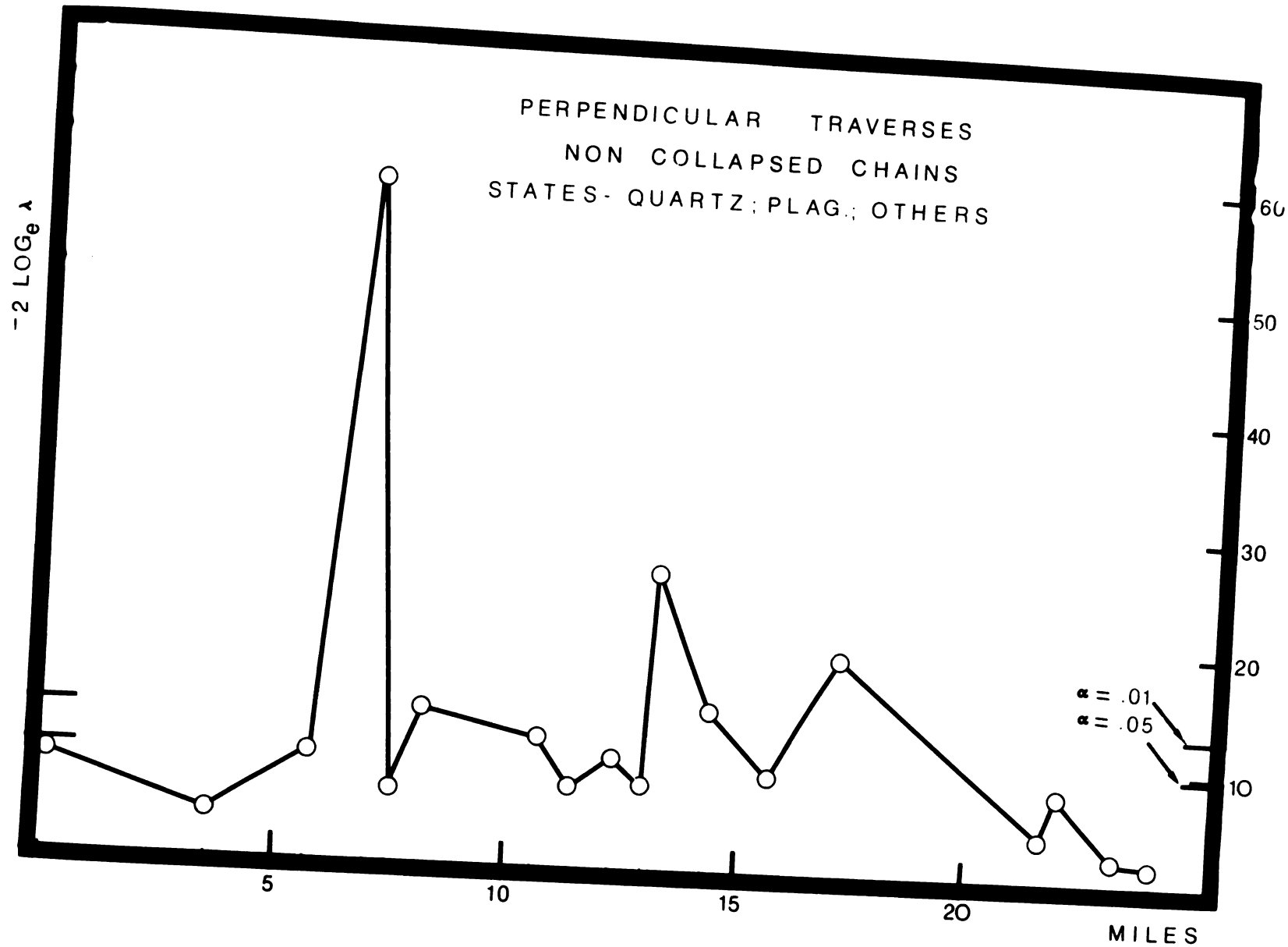
PERPENDICULAR TRAVERSES
NON COLLAPSED CHAINS
STATES- QUARTZ; PLAG.; OTHERS
$-2 \log_e \lambda$
60
50
40
30
20
10
$\alpha = .01$
$\alpha = .05$
5
10
15
20
MILES

plagioclase and others (alkali-feldspar and mica). Examination at the $\alpha = .01$ level shows a mixture of random and non-random association, with sample sites 4, 13 and 18 showing high levels of determinism in their textures, while others are relatively subdued.

Inspection of some observed data points for sample site 1 (low $-2\ln \lambda$ value) and site 4 (high value) explain the large variability in determinism. For site 1, an example traverse was: 12323313221; for site 4: 21111211111. The runs of quartz observations at site 4 are a function of grain size. Larger-than-average quartz grains receive a proportionately larger number of cross-hairs of the test transect. The effect of runs generated by large-sized grains on the transition frequency and transition probability matrices is to "load-up" the diagonal cells. Such an effect is seen in the transitions at site 4:

	QTZ.	PLAG.	OTHER	
QTZ.	82	21	17	120
PLAG.	25	18	11	54
OTHER	16	15	45	76
	123	54	73	
	.492	.216	.292	

The large frequency of quartz-quartz contacts, and other-other contacts is due to the relatively large grain sizes in quartz and alkali-feldspar, respectively. Since 250 transitions are taken per

directional traverse, inflation of like-like cell values, leads to diminution of the off-diagonal α-β cells. It is this grain-size effect which produces a "premature" and abnormally high amount of determinism.

Explanation of the effect of grain size on the test statistic for Markovity is provided by the mosaic model (Figure 18). Traverses taken parallel to the fabric, Figure 19, show similar perturbations in $-2\ln \lambda$ due to grain size. We should be able to expect, in the conversion of an arkose to a meta-arkose, that initially rounded or semi-rounded quartz and alkali feldspar grains would become more distended through tectonism , so that progressively elliptical shapes would be produced as distance up the gradient increases. (The effect of such shape changes on traverse observations parallel to the fabric, is to increase the likelihood of "runs", and hence increase $-2\ln \lambda$.)

Comparison of Figures 17 and 19 shows high values for site 4 for both traverses. The implication is that large grain sizes affected both test directions, and that those grains are relatively well-rounded, since the G-statistic values are nearly the same for both perpendicular and parallel tests. For sites 11, 18, 24, 23 and 20, a substantially higher parallel test value indicates a significant flattening of the overall phase shape. For site 11, this is a flattening of both quartz and alkali feldspar. For sites at the

Figure 18. Model of anticipated levels of textural determinism as a function of distance up the regional gradient.

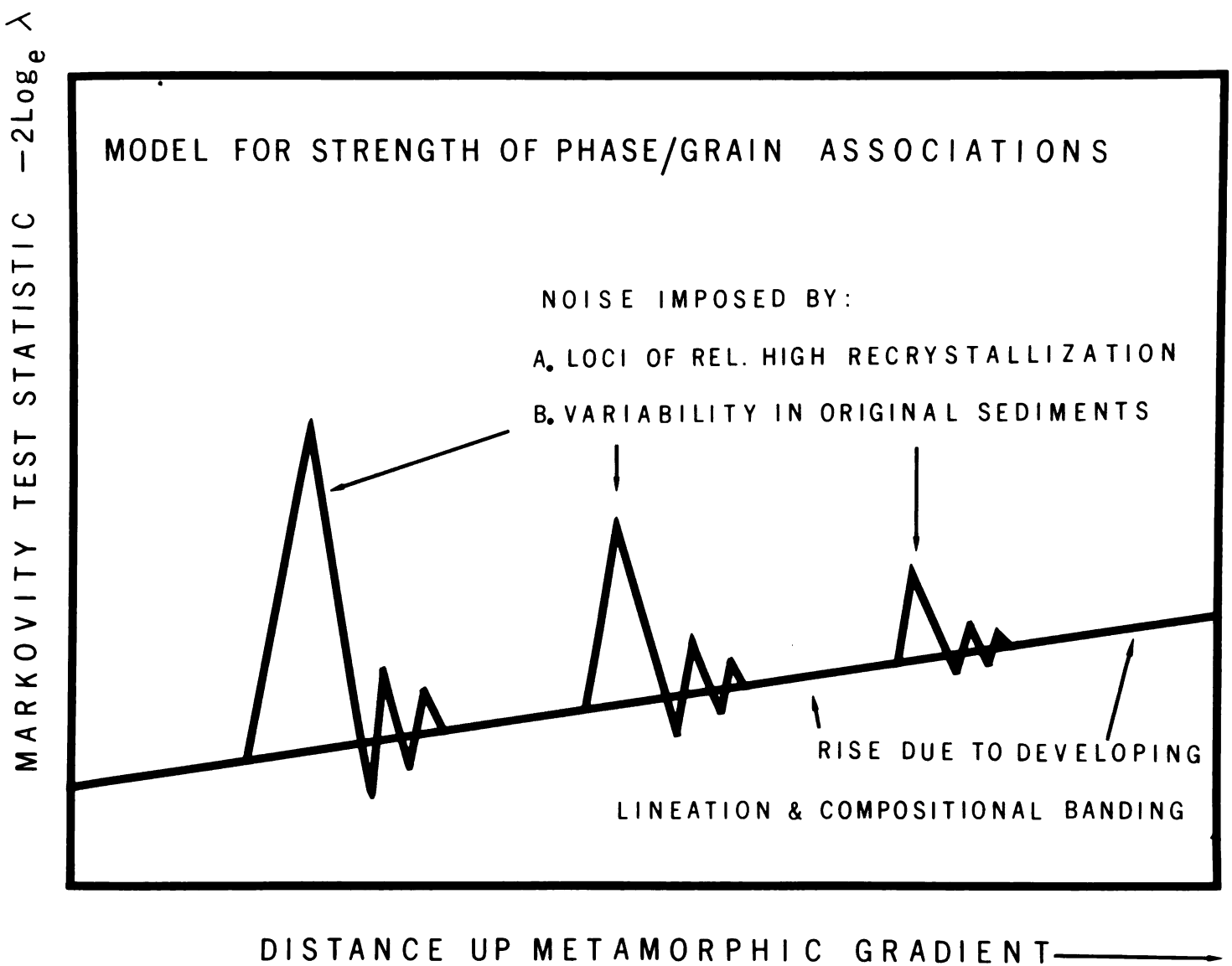
MARKOVITY TEST STATISTIC $-2\text{Log}_e \lambda$
MODEL FOR STRENGTH OF PHASE/GRAIN ASSOCIATIONS
NOISE IMPOSED BY:
A. LOCI OF REL. HIGH RECRYSTALLIZATION
B. VARIABILITY IN ORIGINAL SEDIMENTS
RISE DUE TO DEVELOPING
LINEATION & COMPOSITIONAL BANDING
DISTANCE UP METAMORPHIC GRADIENT

Figure 19. Development of determinism in rock texture as a function of distance up the regional gradient.

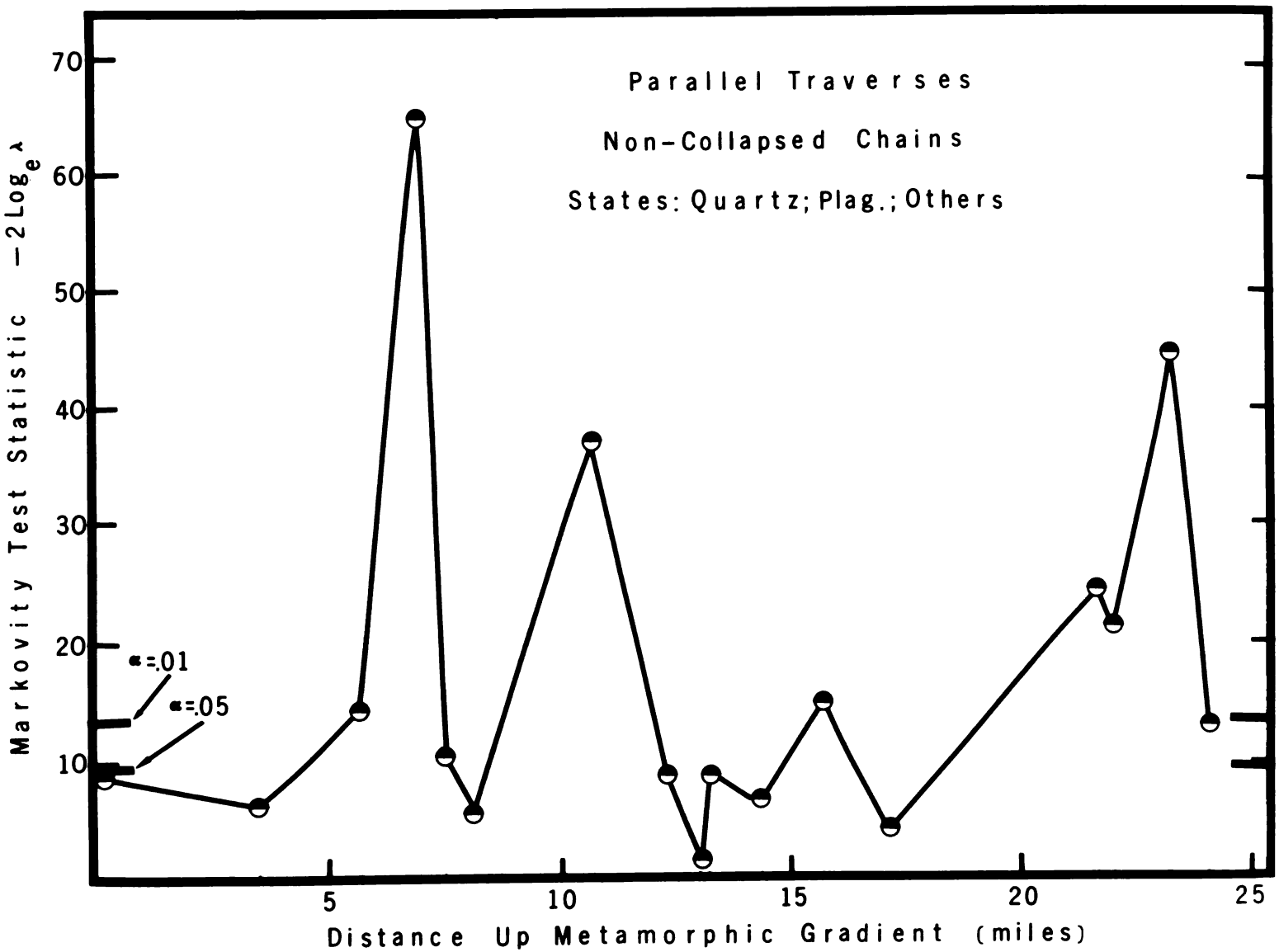
Parallel Traverses
Non-Collapsed Chains
States: Quartz; Plag.; Others
Markovity Test Statistic $-2\text{Log}_e\lambda$
70
60
50
40
30
20
10
α=.01
α=.05
5
10
15
20
25
Distance Up Metamorphic Gradient (miles)

higher-grade end, i.e. 18, 24, 23, and 20, the flattening is primarily in quartz, since alkali feldspar begins breaking down to brown biotite at the staurolite isograd (about site 15). Such distensions in the over-all quartz phase are likely recrystallization adjustments to applied stress.

COLLAPSED CHAINS

The noise imposed on the -2ln λ spectrum by grain-size effects may be removed by collapsing the observation chain (25). Such collapsing provides a means of examining the strength of association between unlike phases. Indeed, this kind of textural information may only be abstracted through the collapsing process.

Sample traverses presented earlier were: 12323313221, and 21111211111, from sites 1 and 4 respectively. Their collapsed forms are 123231321, and 2121 respectively.

It is important to note that the collapsing operation produces an "artificial" texture of unit grain size, and, of course, one without like-like (α-α) grain boundaries. It must, therefore, be evaluated in conjunction with the non-collapsed results for evaluation of the "real" texture.

The effect of collapsing on the transition frequency matrix reduces the diagonal (like-like) cell frequencies to zero. The frequency matrix for site 4 (perpendicular testing) now looks like:

	QTZ.	PLAG.	OTHER
QTZ.	0	21	17
PLAG.	25	0	11
OTHER	16	15	0

.

Elimination of non-zero diagonal elements throws all the probability of state-state transitions into the off-diagonal cells in the transition probability matrix:

	Q	PL.	O
Q	0	.710	.289
PL.	.820	0	.179
O	.473	.526	0

This results in relatively large -2ln λ values, and strongly deterministic "textures", as in Figure 20.

Kullback, et al. (1962) have reported that specification of zero-valued elements under the null hypothesis will reduce the number of degrees of freedom by one for each zero. This is in agreement with Pielou (1965). This causes a drop in degrees of freedom from four to two for comparison of -2ln λ with X^2.

Substantial site-to-site variation occurs in the strengths of phase associations. Comparison of a low -2ln λ at site 4 and a high value at site 6 reveals as much variation in large-scale textural phase associations as in nearly all 24 miles of prograde traverse. Examination of transition frequency matrices for non-collapsed

Figure 20. Development of determinism in rock texture as a function of distance up the regional gradient.

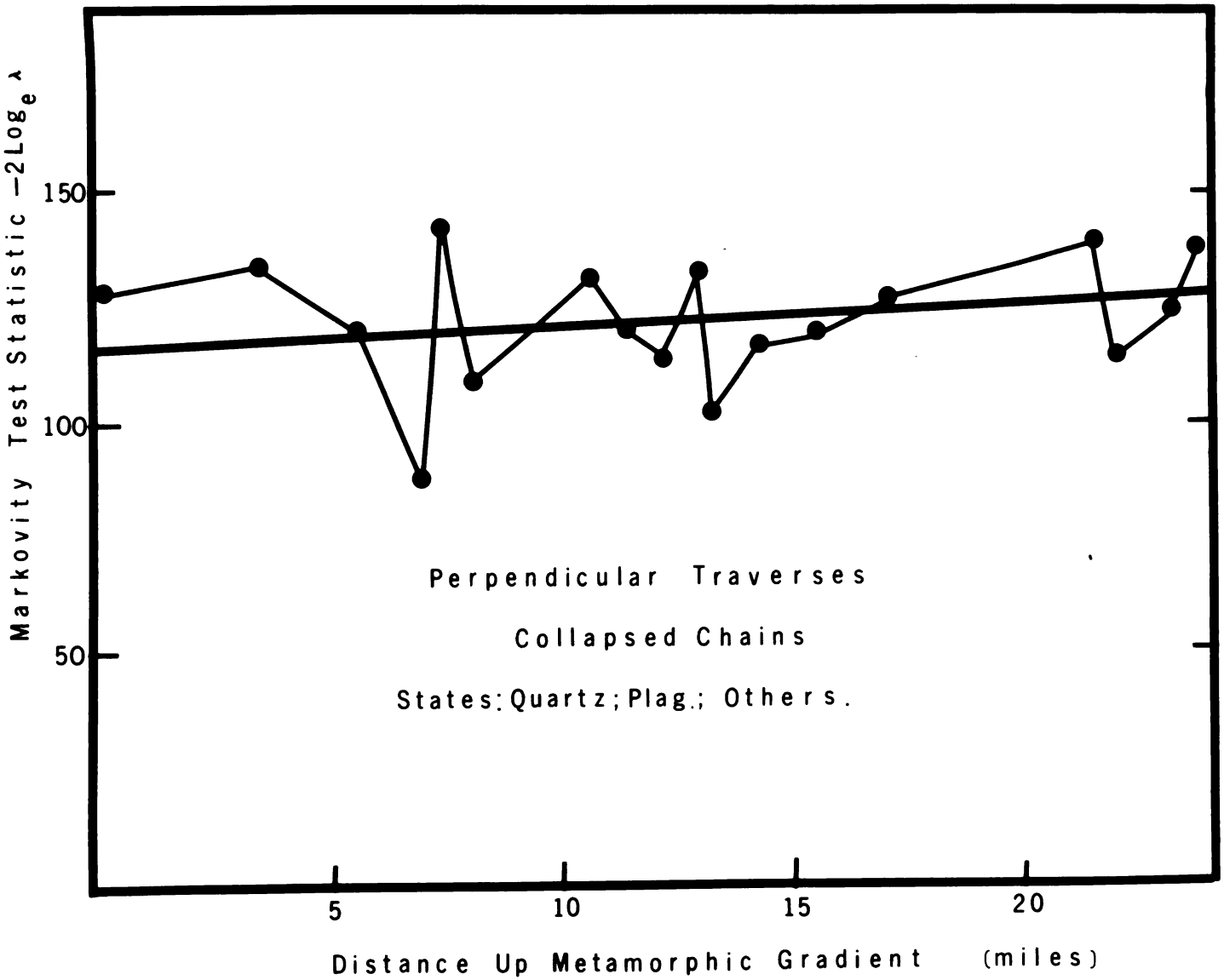
Markovity Test Statistic $-2\text{Log}_e\lambda$
150
100
50
Perpendicular Traverses
Collapsed Chains
States: Quartz; Plag.; Others.
5
10
15
20
Distance Up Metamorphic Gradient (miles)

treatments of sites 4 and 6 reveal a substantial number of long alkali feldspar "runs" at site 4, and a significant decrease in run length at site 6. The reduction in alkali feldspar grain size between sites permitted a relative increase in the number of quartz-other plagioclase-other contacts in samples gathered at site 6. This α-β type contact increase resulted in an increase in Markov character between sites 4 and 6.

Removal of alkali feldspar from the "others" state, and a lumping with plagioclase to form the state "feldspar" permits a new comparison to be made (Figure 21). Dashed lines tracing the values of $-2\ln \lambda$ for quartz-feldspar-others chains, closely correspond to values for non-lumped quartz-plagioclase-others. Departure from good fit occurs, however, between sites 15 to 18 inclusive. Examination of the transition frequency matrices shows a large conditional probability shift from column 3 (others) to column 2 (feldspar) when comparisons of the non-lumped and lumped formats at site 15 are made. This results from the removal of an appreciable number of transitions involving alkali feldspar from "others", and insertion in "feldspar". As K-feldspar continues to break down to biotite the departure from fit lessens, and good agreement is restored by site 24, indicating absence of alkali feldspar from the rock fabric.

Figure 21. Levels of determinism in rock texture for two formats of aggregates as a function of distance up the regional gradient.

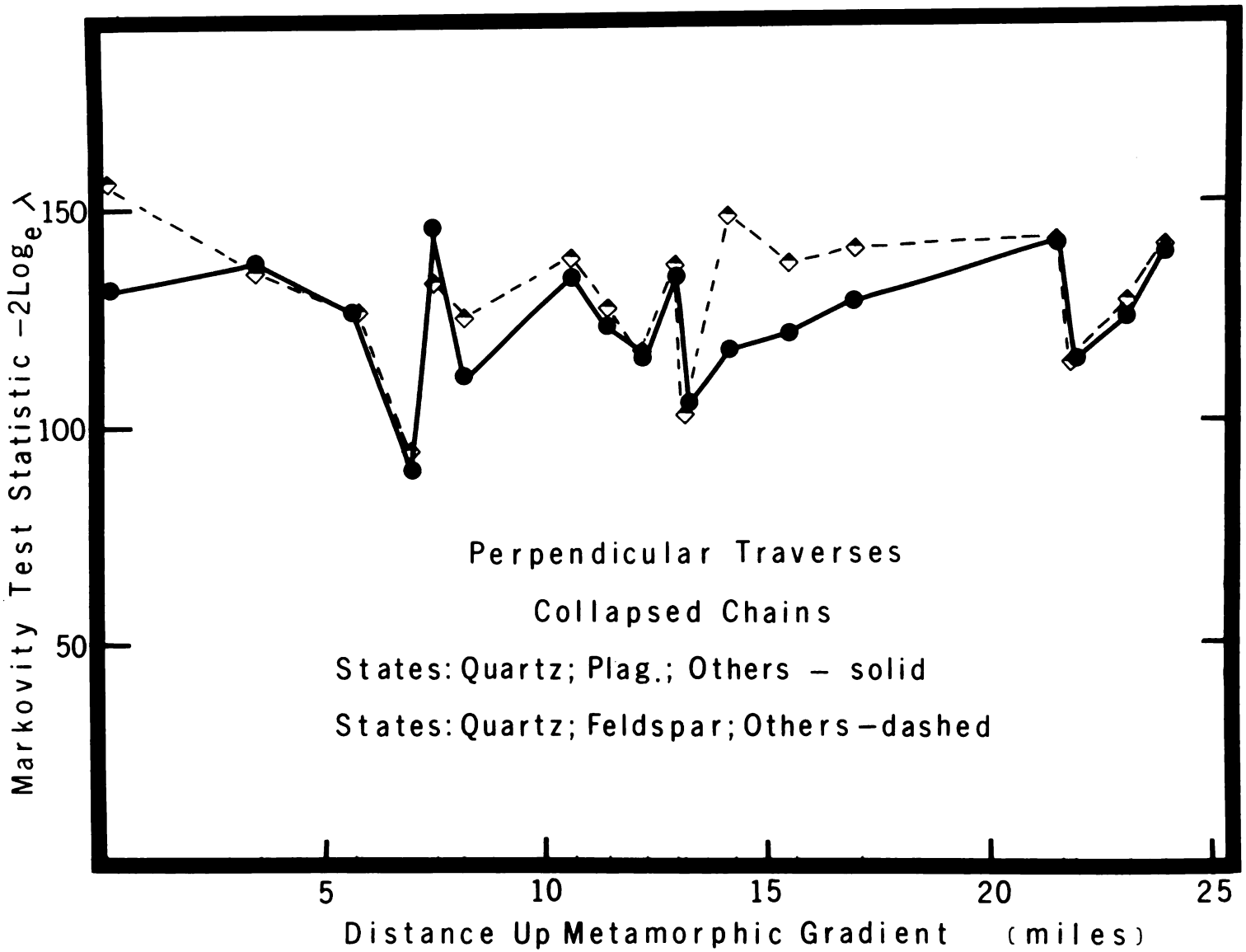
Markovity Test Statistic $-2\text{Log}_e\lambda$
150
100
50
Perpendicular Traverses
Collapsed Chains
States: Quartz; Plag.; Others – solid
States: Quartz; Feldspar; Others – dashed
5
10
15
20
25
Distance Up Metamorphic Gradient (miles)

Plotting a "best-fit" straight line through values of $-2\ln \lambda$, for both coding formats, does not provide the overall increase initially suspected (Figure 22). H_o: $\beta = 0$ for the regression equation is not rejected at $\alpha = .05$ with 16 degrees of freedom. It is of interest to note, however, that departures from this best fit line reduce with distance up the metamorphic gradient. For both coding formats, the reductions are comparable in magnitude. Hence, it appears that collapsed-chain textural determinism may approach some limiting value. This suggests classic stochastic convergence.

CONCLUSIONS

We have presented models to predict changes in surface area and changes in neighborhood mosaic patterns with increased metamorphic grade.

Results of several analyses of variance indicate that substantial variation in both the like (α-α) and unlike (α-β) components of surface area can occur in quartz within a single sample site. This indicates that quartz surface area may be too sensitive a parameter for regional comparisons of recrystallization and grain growth. Significant differences in both the components of plagioclase surface area between sample sites indicate that plagioclase may be most suited for regional comparisons. This is in general agreement with the results of an earlier study (1).

Figure 22. Bouncing level of determinism in rock texture as a function of distance up the regional gradient.

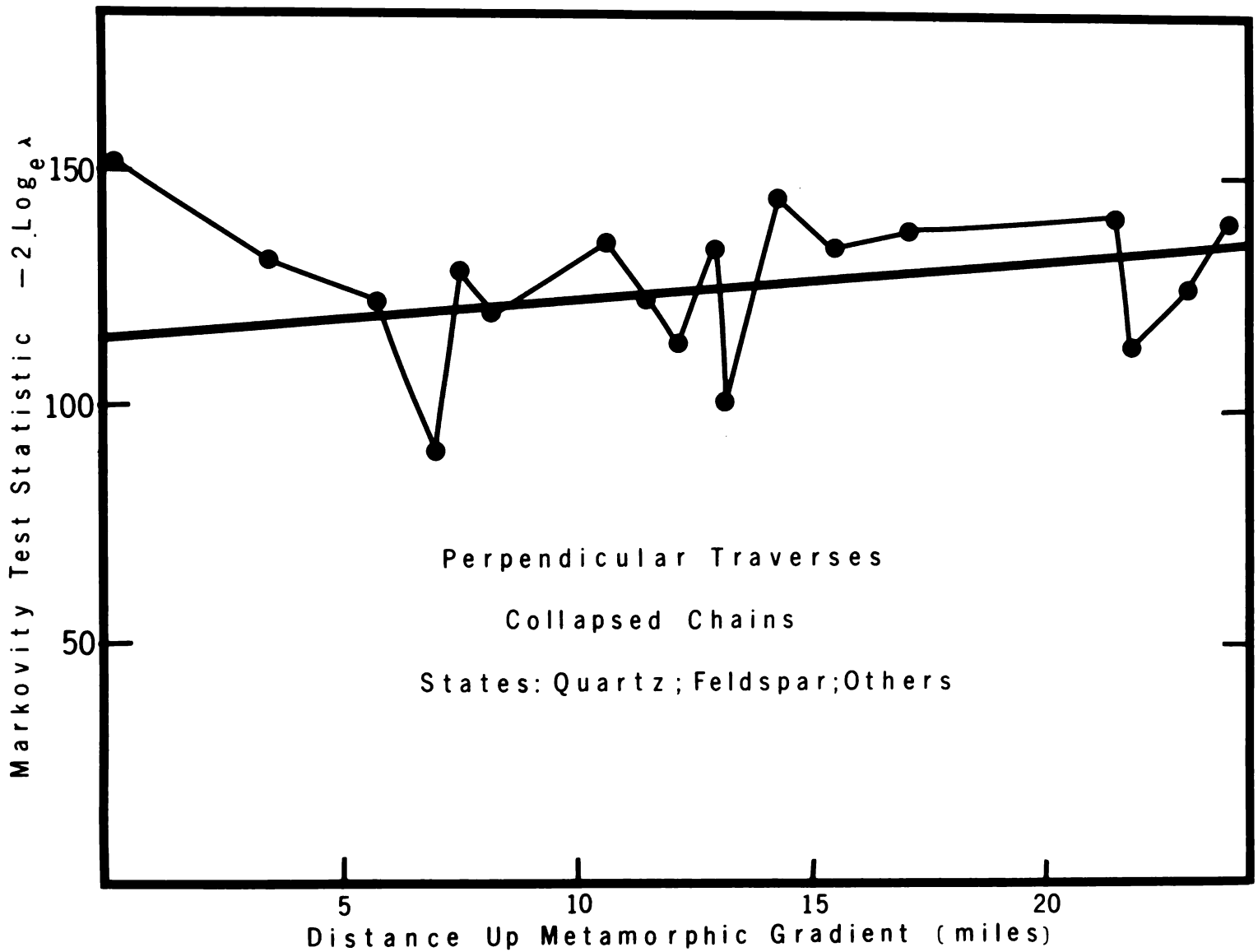
Markovity Test Statistic $-2 \log_e \lambda$
150
100
50
Perpendicular Traverses
Collapsed Chains
States: Quartz ; Feldspar ; Others
5
10
15
20
Distance Up Metamorphic Gradient (miles)

Results of the least-squares regression of the two components of surface area, and the evaluation of the residuals from regression, indicates that the ratio of like (α-α) to unlike (α-β) surface area does not change linearly with increased metamorphic grade. This is true for both quartz and plagioclase. Higher order terms in the regression equation appear necessary to account for the sinusoidal behavior of the surface area ratios with increased metamorphic grade.

It appears that the contributions of initial sedimentary facies (in terms of pelitic interbedding) and local stress fields may explain variations in surface area not explained by the regression of one component on another.

Textural mosaics were investigated by permitting phases to simulate states in a first-order Markov chain. The rock fabric was examined in directions perpendicular and parallel to the anisotropy of mineral phases.

For non-collapsed chains, grain size variation in quartz and alkali feldspar influenced the amount of Markovity, or determinism of phases in the rock fabric.

Removal of grain-size effects by chain collapsing, permitted the examination of neighborhood changes induced by regional metamorphism. This examination suggests that a limiting value exists for the strength of neighborhood phase associations, and that values obtained

at individual sample sites converge on this limit in a stochastic manner with increasing metamorphic grade.

This work represents a pilot study in a long-range project. It has attempted to outline some of the problems confronting textural work in regional metamorphic environments.

From the results of this study, we suggest:

1) Future work to define the effects that small-scale variations in sedimentary facies, and local variations in the stress field, have on surface area.
2) Increased reliance on approaches which examine all components of variance.
3) Future work to investigate the capabilities of Markov approaches to textural mosaics.
4) Efforts to couple the solid-state physics (i.e.: micromechanics, diffusional processes and associated creep) with small-scale textural evaluations (statistically augmented) on an outcrop scale.

REFERENCES

1) Ehrlich, et al., 1972, Textural variation in petrographic analyses: Geological Society of America Bulletin, V. 83, p. 665-676.

2) Allen, G.C. and Ragland, P.C., 1972, Chemical and mineralogic variations during prograde metamorphism, Great Smoky Mountains, North Carolina-Tennessee: Geological Society of America Bulletin, V. 83, p. 1285-1298.

3) King, P.B., 1964, Geology of the central Great Smoky Mountains, Tennessee: U.S. Geol. Survey Prof. Paper 349-c, 148p.

4) Chapman, D.F., 1968, Petrology, structure and metamorphism of a Granodiorite gneiss in the Grenville Province of southeastern Ontario (Ph.D. dissertation): New Brunswick, New Jersey, Rutgers University.

5) DeVore, G.W., 1959, Role of minimum interfacial free energy in determining the macroscopic features of mineral assemblages. I. The model: Journal of Geology, V. 67, p. 211-227.

6) Cahn, R.W., 1970, Recovery and recrystallization in Physical Metallurgy: Amsterdam, North-Holland Pub. Co.

7) Flinn, D., 1969, Grain contacts in crystalline rocks: Lithos, V. 3, p. 361-370.

8) DeVore, G.W., 1968, Preferred mineral distributions of poly-mineralic rocks related to non-hydrostatic stresses as expressions of mechanical equilibria: Journal of Geology, V. 77, p. 26-38.

9) Burke, J.E., 1968, Grain growth, in Ceramic Microstructures, Fulrath, R.M. and Pask, J.A., New York, John Wiley and Sons.

10) Gordon, P. and Vandermeer, R.A., 1966, Grain boundary migration in Recrystallization, Grain Growth and Textures: A.S.M. conference volume, Cleveland, Ohio.

11) Bailey, E.H. and Stevens, R.E., 1960, Selective staining of k-feldspar and plagioclase on rock slabs and thin sections: American Mineralogist, V. 45, p. 1020-1025.

12) Rack, H.J. and Newman, R.W., 1970, Microstructures, in Physical Metallurgy, Amsterdam, North-Holland Pub. Co.

13) Underwood, E.E., 1970, Quantitative Stereology: Reading, Massachusetts, Addison-Wesley Pub. Co.

14) DeHoff, R.T. and Rhines, F.N., 1968, Quantitative Microscopy: New York, McGraw-Hill Book Co.

15) Sokal, R.R. and Rohlf, F.J., 1969, Biometry: San Francisco, W.H. Freeman & Co.

16) Griffiths, J.C., 1967, Scientific method in the analysis of sediments: New York, McGraw-Hill Book Co.

17) Draper, N.R. and Smith, H., 1966, Applied regression analysis: New York, John Wiley and Sons.

18) Hadley, J.B. and Goldsmith, R., 1963, Geology of the eastern Great Smoky Mountains, North Carolina-Tennessee: U.S. Geological Survey Prof. Paper 349-b, 118p.

19) Vistelius, A.B., 1966, Genesis of the Mt. Belaya granite--an experiment in stochastic modeling: Doklady Akademii Nauk SSSR, V. 167, p. 48-50.

20) Kretz, R., 1969, On the spatial distribution of crystals in rocks: Lithos, V. 2, p. 39-66.

21) Howard, R.A., 1971, Dynamic probabilistic systems, Vol. I: Markov Models: New York, John Wiley and Sons.

22) Kemeny, J.G. and Snell, J.L., 1960, Finite Markov chains: Princeton, N.J., D. Van Nostrand Co.

23) Anderson, T.W. and Goodman, L.A., 1957, Statistical inference about Markov chains: Ann. Math. Stat., V. 28, p. 89-110.

24) Pielou, E.C., 1965, The concept of randomness in the patterns of mosaics: Biometrics, V. 21, p. 908-920.

25) Harbaugh, J.W. and Bonham-Carter, G., 1970, Computer simulation in geology: New York, John Wiley and Sons.

26) Kupperman, Kullback and Ku, 1962, Tests for contingency tables and Markov chains: Technometrics, V. 4, No. 4, p. 573-608.

27) Clarke, A.B. and Disney, R.L., 1970, Probability and random processes for engineers and scientists: New York, John Wiley and Sons.

28) Tsokos, C.P., 1972, Probability distributions: An introduction to probability theory with applications: Belmont, California, Duxbury Press, Wadsworth Publishing.